the product amplified with a sense primer S-E1, specific for LMP7-E1, together with the AS-E1/E2 primer (956 bp) was undetectable (Fig. 1B, bottom). Inability of the primer pair S-E1/AS-E1/E2 to amplify the corresponding DNA fragment was excluded, because both LMP7-E1 and -E2 fragments were efficiently as well as simultaneously amplified when the mixture of equal amount of two plasmids encoding LMP7-E1 and -E2, respectively, was used as templates (Fig. 1B, bottom). Importantly, both IFN-γ-treated parental DLD-1 and DOX-treated DLD-1/TR-IRF-1-tag cells exhibited significant induction of the LMP7-E2 expression, whereas the change of the levels of LMP7-E1 was not observed. These data indicated that LMP7 mRNA, induced by either IFN-γ or forced expression of IRF-1 in DLD-1 cells, mainly consists of the transcript LMP7-E2.

3.3. *IRF-1-dependent transcription of the LMP7 gene leads to expression of the processed form of LMP7 protein*

It was shown that, by using HeLa cells, the LMP7-E2 transcript gives rise to a precursor protein of 28.5 kDa which is subsequently processed into an end product of 23 kDa [26]. When the whole cell extracts from DLD-1 cells before and after IFN-γ treatment (24 h) were examined, the protein product of approximately 23 kDa became visible upon IFN-γ treatment (Fig. 2). The size of this product corresponded to that of a band observed in extracts from IFN-γ-treated HeLa cells, indicating that not only sufficient translation but also the following protein processing of LMP7 could be operational in DLD-1 cells (Fig. 2). Interestingly, the conditional expression of IRF-1 in DLD-1/TR/IRF-1-tag cells also resulted in the induction of the 23-kDa protein, clearly showing that the activation of IRF-1 alone could be enough for the generation of the processed form of LMP7 (Fig. 2).

3.4. *IFN-γ induces the binding of IRF-1 to the region +291/+747 of the human LMP7 gene*

The putative binding sites for several transcription factors were noted on a limited region approximately 800 bp upstream of the exon 1 of the human LMP7 gene [26]. However, the functional relevance of the transcriptional regulation to any specific sequences within or in the proximity of this region has remained undetermined. Therefore, we next tested whether IRF-1 directly interacts with the 5′ flanking or intragenic region of the LMP7 gene by using ChIP assays with chromatin extracts of DLD-1 cells [24]. We designed six pairs of PCR primers to amplify DNA fragments of ~400 bp each, attempting to analyze the genomic region of approximately ~2.5 kb in total that extends both upstream and downstream of the transcription start site of the LMP7-E1 (+1) (Fig. 3A, top). In the absence of IFN-γ, the specific binding of IRF-1 to this region appeared to be scarce, because anti-IRF-1 antibody precipitated only small amount of any fragment throughout the region (Fig. 3A, middle). By contrast, when cells were stimulated with IFN-γ, a significant induction of the promoter occupancy by IRF-1 was observed particularly within the region +291 to +747 (Fig. 3A, middle). These results suggested that, upon stimulation with IFN-γ, IRF-1 interacts with certain binding sites within the sequence from +291 to +747 and activates the LMP7 gene transcription. Indeed, a search for potential binding sequences for the IRF family protein in the entire region of ~2.5 kb revealed a single sequence GCTTTCGCTTTC at +581/+592, which completely matches IRF-E consensus sequence, within the region from +291 to +747. We also found four other potential sequences that incompletely match the consensus IRF-E within this region; one having two nucleotide mismatches and a nucleotide deletion at +1417/+1427, and the others having three nucleotide mismatches at −700/−689, +411/+422 and +513/+524. However, from our ChIP data, we concluded that these sites do not serve as critical binding sites for IRF-1 in response to IFN-γ stimulation.

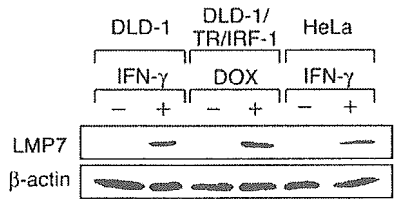

Fig. 2. IRF-1 induces expression of the processed form of LMP7 protein. Parental DLD-1 (DLD-1) and HeLa cells, or DLD-1/TR/IRF-1-tag (DLD-1/TR/IRF-1) cells were stimulated with IFN-γ (50 ng/ml) or DOX (100 ng/ml), respectively, and were collected before and after 24 h of stimulation. Eighty micrograms of DLD-1 and DLD-1/TR/IRF-1 cell extracts or 160 μg of HeLa cell extracts were subjected to Western blot analysis. Immunoblot was initially performed with an anti-LMP7 antibody and then followed by reprobing with an anti-β-actin antibody.

3.5. *Both IFN-γ and IRF-1 enhance the transcriptional activity of the LMP7 gene via the IRF-E at +581/+592*

To ascertain the functional involvement of the IRF-E at +581/+592 in the LMP7 gene transcription, we constructed a reporter plasmid carrying the region −100 to +1601 (LMP7-wt-Luc). When HeLa cells were transiently transfected with the plasmid and assayed, the reporter activity was significantly induced in response to IFN-γ (Fig. 3B). When a mutated version of the reporter gene (LMP7-mt-Luc), defective in binding to IRF proteins due to a 4-bp mutation in the IRF-E, was analyzed in parallel, the IFN-γ-dependent induction of reporter activity was significantly lower than that of the wild-type LMP7-Luc (Fig. 3B). Interestingly, when assessed by cotransfecting an expression vector encoding IRF-1, the forced expression of IRF-1 resulted in a significant enhancement of the transcriptional activity of the LMP7-wt-Luc, while it had little effect on that of the LMP7-mt-Luc. Similar results were obtained when the same series of experiments were carried out by using DLD-1 cells, although the luciferase activities were extremely lower than those in HeLa cells, probably reflecting the low efficiency of transfection (data not shown). Taken together, it was indicated that the IRF-E at +581/+592 and its interaction with IRF-1 are functionally important for inducible expression of the human LMP7 gene by IFN-γ.

3.6. *Silencing IRF-1 results in marked reduction of the IFN-γ-dependent LMP7 protein expression*

To address the involvement of IRF-1 in LMP7 expression more directly, we next performed transient transfection experiments of an IRF-1-specific siRNA oligonucleotide into DLD-1 and HeLa cells and assessed its influences on LMP7 expression (Fig. 4). In our experimental system, the expression of IRF-1 protein was suppressed by its specific siRNA to ~20% of the control in DLD-1 and to undetectable level in HeLa

cells, respectively, even after the stimulation with IFN-γ (Fig. 4). Again, the difference in the potency of the siRNA treatment was assumed to be due to that in the transfection efficiency between these cell types. As expected, reprobing the same blots with anti-LMP7 antibodies revealed that the expression of LMP7 upon IFN-γ treatment was decreased below the detection levels in both cell types (Fig. 4). These data clearly indicated that IRF-1 plays a major role in linking the IFN-γ action to the resultant expression of LMP7 protein.

3.7. *IRF-1 functions as a critical mediator for IFN-γ-dependent expression of LMP7, LMP2 and MECL1 in vivo*

The 5′ part of the human and murine LMP7 genes shows the approximately 290 bp region containing the IRF-E to be highly conserved. Based on this notion, we assessed the role of IRF-1 in LMP7 expression in vivo by using IRF-1−/− or wild-type

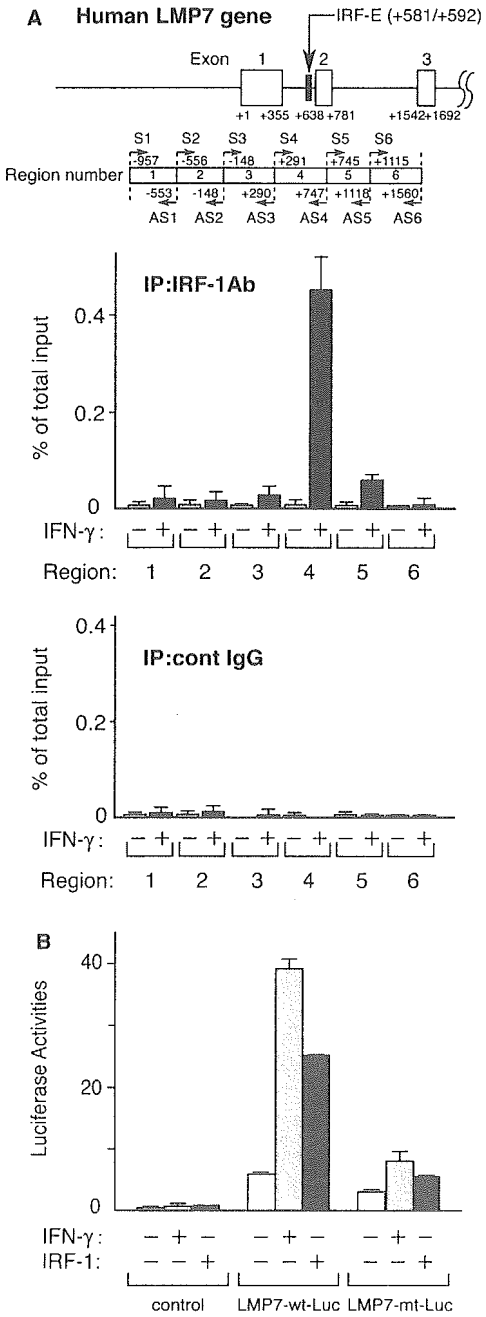

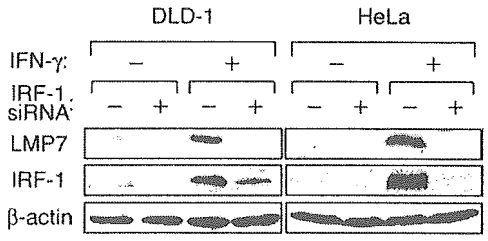

Fig. 4. Silencing IRF-1 expression by its specific siRNA results in marked reduction of LMP7 protein expression. Parental DLD-1 and HeLa cells were transfected with either siRNA oligonucleotides targeting IRF-1 (+) or control siRNA (−). After transfection, cells were cultured under the usual conditions for an additional 12 h and then cultured in the presence (+) or absence (−) of IFN-γ (50 ng/ml). Cells were lysed after 24 h, and 80 μg of DLD-1 extracts or 160 μg of HeLa extracts were subjected to Western blot analysis. Immunoblot was performed with an anti-LMP7 antibody and sequentially followed by reprobing with an anti-IRF-1 and an anti-β-actin antibody.

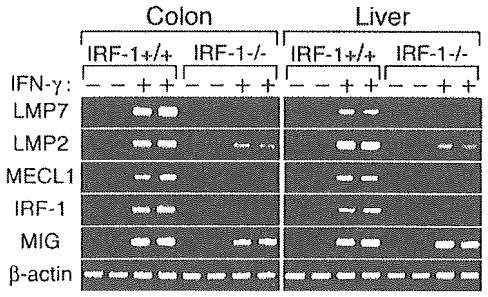

Fig. 5. IRF-1 functions as a critical mediator for IFN-γ-dependent expression of LMP7, LMP2 and MECL1 in vivo. IRF-1−/− and wild-type (IRF-1+/+) mice were injected i.p. with either murine IFN-γ (1×10^5 U/mouse) or vehicle alone ($n = 2$ per group). After 6 h of injection, total RNAs from colon and liver tissues were isolated and analyzed by semi-quantitative RT-PCR for LMP7, LMP2, MECL1, IRF-1, MIG and β-actin. PCR products were electrophoresed and visualized by ethidium bromide staining. Each lane represents a sample from an individual mouse.

control mice (Fig. 5). After intraperitoneal injection of mice with murine IFN-γ or sterile vehicle alone, total RNAs extracted from the colon and liver were subjected to semi-quanti-

Fig. 3. IRF-1 binds to the region +291/+747, and the IRF-E at +581/+592 within this region functions as a critical enhancer element in human LMP7 gene transcription. (A) The genomic regions analyzed by the ChIP assays were schematically shown with the 5′ part of the human LMP7 gene (top). Six pairs of the primers and each PCR-amplified region were indicated with numbers through 1 to 6. Nucleotide numbers were given as shown in Fig. 1B. The location of a consensus sequence for IRF-E is also indicated (top). DLD-1 cells were treated with IFN-γ (50 ng/ml) or left untreated for 6 h and processed for ChIP assays by using anti-IRF-1 antibody (middle) or control IgG (bottom). Precipitated DNA was analyzed by quantitative PCR to amplify each of six regions shown in the top panel. The amount of immunoprecipitated fragment relative to that present in total input chromatin (% of total input) was calculated as described in Section 2. Data are shown as the means ± S.D. of three independent chromatin immunoprecipitations. (B) Either 5 μg of a pGL3-basic (control), LMP7-wt-Luc or LMP7-mt-Luc was transiently transfected into HeLa cells along with 0.03 μg of a *Renilla* luciferase reporter pRL-TK-Luc. One hundred nanograms of an expression vector pcDNA3-IRF-1 was also cotransfected and the total amounts of DNA were adjusted by adding the same amount of an empty expression vector. Cells were cultured in the presence or absence of IFN-γ (50 ng/ml) for 24 h, and the cellular lysates were assayed for reporter activities. Results are the means ± S.D. of three independent experiments.

tative RT-PCR. In both tissues of the wild-type mice treated with IFN-γ, the levels of IRF-1 expression were significantly higher than those of the mice treated with the vehicle alone (Fig. 5). Furthermore, expressions of three immunosubunits of the proteasome, LMP7, LMP2 and MECL1, and also of MIG, known as an inducible gene by IFN-γ, were significantly increased in IFN-γ-treated wild-type mice in both tissues (Fig. 5). In striking contrast, in IRF-1−/− mice, virtually no induction of LMP7 and MECL1, or only a little induction of LMP2 was detected in response to IFN-γ (Fig. 5). We could verify the effects of IFN-γ in IRF-1−/− mice, because the upregulation of MIG in response to IFN-γ in IRF-1−/− mice was comparable to that in wild-type mice, reflecting the dependence of its transcription not on IRF-1 but on other signaling pathways downstream of the IFN-γ action [29,30]. In addition, it seemed reasonable that the expression of LMP2 was to some extent upregulated by IFN-γ in IRF-1−/− mice, because its expression was mediated by both IRF-1-dependent and -independent mechanisms, the latter of which involves activation of signal transducer and activator of transcription (STAT) proteins [19,20]. Taken together, these data demonstrated that IRF-1 serves as a critical regulator for IFN-γ-mediated LMP7 expression in parallel with its role in the induction of LMP2 and MECL1 by IFN-γ in vivo.

4. Discussion

In this study, we provide the evidence that IRF-1 plays a central role in the transcriptional regulation of the LMP7 gene by taking several experimental approaches. It was demonstrated that, by using siRNA-mediated gene silencing experiments, IRF-1 mediates IFN-γ-dependent LMP7 expression in both DLD-1 and HeLa cells that are derived from different tissues of human origin. Additionally, we showed essential roles of IRF-1 in IFN-γ-dependent LMP7 gene expression by analyzing two different murine tissues. Together with the fact that the genomic region surrounding the IRF-E of the human LMP7 gene is highly conserved with that of murine one, it was strongly suggested that the mechanism of LMP7 gene transcription by IRF-1 might be broadly conserved beyond the cell types and the species.

Our study also demonstrated that not only mRNA but also the processed protein product of LMP7 was efficiently induced by the overexpression of IRF-1, which was irrespective of the IFN-γ action. This suggests that various signaling pathways or the target molecules that are activated by IFN-γ, other than IRF-1, have little, if any, effect on the following protein processing of LMP7. It was previously indicated that the processed form of the LMP7 protein could be readily generated only if an expression plasmid for the LMP7-E2 was transfected into HeLa cells [26,28]. These collective findings emphasize that the cleavage of the precursor protein at its N-terminal site is regulated by a certain yet unidentified mechanism preexisting in most cell types, and that the most critical step for the expression of functionally matured LMP7 protein may be its transcriptional regulation by IRF-1.

Early studies analyzing the effect of solely overexpressed LMP7 in several cell lines yielded somewhat discordant results with respect to the change of the cleavage specificity of the 20S proteasome [11,31,32]. However, it has been becoming obvious that the entire function of LMP7 on antigen processing may not be simply accounted for by its own catalytic activity. For example, recent studies have shown that the assembly of the immunoproteasome consists of complex processes that require interdependent incorporation of the three IFN-γ-inducible subunits, and that LMP7 contributes to the maturation of an intermediate form of the immunoproteasome that contains LMP2 and MECL1 [17]. Indeed, such cooperative mechanism was confirmed by the observation that simultaneous expression of all these three immunosubunits, even at relatively low levels, could process certain epitopes with increased efficiency [33,34]. In addition, the finding that even a catalytically inactive mutant of LMP7 could facilitate a certain epitope generation when expressed in combination with LMP2 and MECL1 [15], via its effect on induction of structural changes of the immunoproteasomes, further support the notion that the concerted presence of the immunosubunits would be essential for maximizing the function of the immunoproteasome. Importantly, recent data have demonstrated that not only IFN-γ but also other factors such as tumor necrosis factor-α (TNF-α) could induce coordinated expression of the three immunosubunits in certain cell types [35]. Together with the notion that IRF-1 could be upregulated by a variety of cytokines such as TNF-α [36] or viral infection [37], we believe the present data that the expression of LMP7 is regulated by IRF-1 in tune with the other two immunosubunits LMP2 and MECL1 would be of significant importance, because this brings forward the central role of IRF-1 in the reorganization of the proteaosomes into immunoproteasomes, serving as a master switch that enables the proper class I antigen processing and the following immune responses in a variety of situations.

Acknowledgements: This study was supported in part by grants-in-aid for Scientific Research, Scientific Research on Priority Areas, Exploratory Research and Creative Scientific Research from the Japanese Ministry of Education, Culture, Sports, Science and Technology; the Japanese Ministry of Health, Labor and Welfare; the Japan Medical Association; Foundation for Advancement of International Science; Terumo Life science Foundation; Ohyama Health Foundation; Yakult Bio-Science Foundation; Research Fund of Mitsukoshi Health and Welfare Foundation.

References

[1] Rock, K.L., Gramm, C., Rothstein, L., Clark, K., Stein, R., Dick, L., Hwang, D. and Goldberg, A.L. (1994) Inhibitors of the proteasome block the degradation of most cell proteins and the generation of peptides presented on MHC class I molecules. Cell 78, 761–771.
[2] Kloetzel, P.M. and Ossendorp, F. (2004) Proteasome and peptidase function in MHC-class-I-mediated antigen presentation. Curr. Opin. Immunol. 16, 76–81.
[3] Martinez, C.K. and Monaco, J.J. (1991) Homology of proteasome subunits to a major histocompatibility complex-linked LMP gene. Nature 353, 664–667.
[4] Glynne, R., Powis, S.H., Beck, S., Kelly, A., Kerr, L.A. and Trowsdale, J. (1991) A proteasome-related gene between the two ABC transporter loci in the class II region of the human MHC. Nature 353, 357–360.
[5] Kelly, A., Powis, S.H., Glynne, R., Radley, E., Beck, S. and Trowsdale, J. (1991) Second proteasome-related gene in the human MHC class II region. Nature 353, 667–668.
[6] Yang, Y., Waters, J.B., Fruh, K. and Peterson, P.A. (1992) Proteasomes are regulated by interferon γ: implications for antigen processing. Proc. Natl. Acad. Sci. USA 89, 4928–4932.
[7] Fruh, K., Gossen, M., Wang, K., Bujard, H., Peterson, P.A. and Yang, Y. (1994) Displacement of housekeeping proteasome subunits by MHC-encoded LMPs: a newly discovered mechanism

for modulating the multicatalytic proteinase complex. EMBO J. 13, 3236–3244.
[8] Nandi, D., Jiang, H. and Monaco, J.J. (1996) Identification of MECL-1 (LMP-10) as the third IFN-γ-inducible proteasome subunit. J. Immunol. 156, 2361–2364.
[9] Hisamatsu, H., Shimbara, N., Saito, Y., Kristensen, P., Hendil, K.B., Fujiwara, T., Takahashi, E., Tanahashi, N., Tamura, T., Ichihara, A. and Tanaka, K. (1996) Newly identified pair of proteasomal subunits regulated reciprocally by interferon γ. J. Exp. Med. 183, 1807–1816.
[10] Driscoll, J., Brown, M.G., Finley, D. and Monaco, J.J. (1993) MHC-linked LMP gene products specifically alter peptidase activities of the proteasome. Nature 365, 262–264.
[11] Gaczynska, M., Rock, K.L., Spies, T. and Goldberg, A.L. (1994) Peptidase activities of proteasomes are differentially regulated by the major histocompatibility complex-encoded genes for LMP2 and LMP7. Proc. Natl. Acad. Sci. USA 91, 9213–9217.
[12] Eleuteri, A.M., Kohanski, R.A., Cardozo, C. and Orlowski, M. (1997) Bovine spleen multicatalytic proteinase complex (proteasome). Replacement of X, Y, and Z subunits by LMP7, LMP2, and MECL1 and changes in properties and specificity. J. Biol. Chem. 272, 11824–11831.
[13] Gileadi, U., Moins-Teisserenc, H.T., Correa, I., Booth Jr., B.L., Dunbar, P.R., Sewell, A.K., Trowsdale, J., Phillips, R.E. and Cerundolo, V. (1999) Generation of an immunodominant CTL epitope is affected by proteasome subunit composition and stability of the antigenic protein. J. Immunol. 163, 6045–6052.
[14] Sewell, A.K., Price, D.A., Teisserenc, H., Booth Jr., B.L., Gileadi, U., Flavin, F.M., Trowsdale, J., Phillips, R.E. and Cerundolo, V. (1999) IFN-γ exposes a cryptic cytotoxic T lymphocyte epitope in HIV-1 reverse transcriptase. J. Immunol. 162, 7075–7079.
[15] Sijts, A.J., Ruppert, T., Rehermann, B., Schmidt, M., Koszinowski, U. and Kloetzel, P.M. (2000) Efficient generation of a hepatitis B virus cytotoxic T lymphocyte epitope requires the structural features of immunoproteasomes. J. Exp. Med. 191, 503–514.
[16] Fehling, H.J., Swat, W., Laplace, C., Kuhn, R., Rajewsky, K., Muller, U. and von Boehmer, H. (1994) MHC class I expression in mice lacking the proteasome subunit LMP-7. Science 265, 1234–1237.
[17] Griffin, T.A., Nandi, D., Cruz, M., Fehling, H.J., Kaer, L.V., Monaco, J.J. and Colbert, R.A. (1998) Immunoproteasome assembly: cooperative incorporation of interferon γ (IFN-γ)-inducible subunits. J. Exp. Med. 187, 97–104.
[18] White, L.C., Wright, K.L., Felix, N.J., Ruffner, H., Reis, L.F., Pine, R. and Ting, J.P. (1996) Regulation of LMP2 and TAP1 genes by IRF-1 explains the paucity of CD8+ T cells in IRF-1−/− mice. Immunity 5, 365–376.
[19] Chatterjee-Kishore, M., Kishore, R., Hicklin, D.J., Marincola, F.M. and Ferrone, S. (1998) Different requirements for signal transducer and activator of transcription 1α and interferon regulatory factor 1 in the regulation of low molecular mass polypeptide 2 and transporter associated with antigen processing 1 gene expression. J. Biol. Chem. 273, 16177–16183.
[20] Brucet, M., Marques, L., Sebastian, C., Lloberas, J. and Celada, A. (2004) Regulation of murine Tap1 and Lmp2 genes in macrophages by interferon gamma is mediated by STAT1 and IRF-1. Genes Immun. 5, 26–35.
[21] Foss, G.S. and Prydz, H. (1999) Interferon regulatory factor 1 mediates the interferon-γ induction of the human immunoproteasome subunit multicatalytic endopeptidase complex-like 1. J. Biol. Chem. 274, 35196–35202.
[22] Kroger, A., Koster, M., Schroeder, K., Hauser, H. and Mueller, P.P. (2002) Activities of IRF-1. J. Interferon Cytokine Res. 22, 5–14.
[23] Taniguchi, T., Ogasawara, K., Takaoka, A. and Tanaka, N. (2001) IRF family of transcription factors as regulators of host defense. Annu. Rev. Immunol. 19, 623–655.
[24] Oshima, S., Nakamura, T., Namiki, S., Okada, E., Tsuchiya, K., Okamoto, R., Yamazaki, M., Yokota, T., Aida, M., Yamaguchi, Y., Kanai, T., Handa, H. and Watanabe, M. (2004) Interferon regulatory factor 1 (IRF-1) and IRF-2 distinctively up-regulate gene expression and production of interleukin-7 in human intestinal epithelial cells. Mol. Cell. Biol. 24, 6298–6310.
[25] Matsuyama, T., Kimura, T., Kitagawa, M., Pfeffer, K., Kawakami, T., Watanabe, N., Kundig, T.M., Amakawa, R., Kishihara, K., Wakeham, A., Potter, J., Furlonger, C.L., Narendran, A., Suzuki, H., Ohashi, P.S., Paige, C.J., Taniguchi, T. and Mak, T.W. (1993) Targeted disruption of IRF-1 or IRF-2 results in abnormal type I IFN gene induction and aberrant lymphocyte development. Cell 75, 83–97.
[26] Fruh, K., Yang, Y., Arnold, D., Chambers, J., Wu, L., Waters, J.B., Spies, T. and Peterson, P.A. (1992) Alternative exon usage and processing of the major histocompatibility complex-encoded proteasome subunits. J. Biol. Chem. 267, 22131–22140.
[27] Paulukat, J., Bosmann, M., Nold, M., Garkisch, S., Kampfer, H., Frank, S., Raedle, J., Zeuzem, S., Pfeilschifter, J. and Muhl, H. (2001) Expression and release of IL-18 binding protein in response to IFN-γ. J. Immunol. 167, 7038–7043.
[28] Yang, Y., Fruh, K., Ahn, K. and Peterson, P.A. (1995) In vivo assembly of the proteasomal complexes, implications for antigen processing. J. Biol. Chem. 270, 27687–27694.
[29] Guyer, N.B., Severns, C.W., Wong, P., Feghali, C.A. and Wright, T.M. (1995) IFN-γ induces a p91/Stat1α-related transcription factor with distinct activation and binding properties. J. Immunol. 155, 3472–3480.
[30] Ohmori, Y. and Hamilton, T.A. (1998) STAT6 is required for the anti-inflammatory activity of interleukin-4 in mouse peritoneal macrophages. J. Biol. Chem. 273, 29202–29209.
[31] Groettrup, M., Ruppert, T., Kuehn, L., Seeger, M., Standera, S., Koszinowski, U. and Kloetzel, P.M. (1995) The interferon-γ-inducible 11 S regulator (PA28) and the LMP2/LMP7 subunits govern the peptide production by the 20 S proteasome in vitro. J. Biol. Chem. 270, 23808–23815.
[32] Kuckelkorn, U., Frentzel, S., Kraft, R., Kostka, S., Groettrup, M. and Kloetzel, P.M. (1995) Incorporation of major histocompatibility complex– encoded subunits LMP2 and LMP7 changes the quality of the 20S proteasome polypeptide processing products independent of interferon-γ. Eur J. Immunol. 25, 2605–2611.
[33] Sijts, A., Standera, S., Toes, R.E., Ruppert, T., Beekman, N.J., van Veelen, P.A., Ossendorp, F.A., Melief, C.J. and Kloetzel, P.M. (2000) MHC class I antigen processing of an adenovirus CTL epitope is linked to the levels of immunoproteasomes in infected cells. J. Immunol. 164, 4500–4506.
[34] Schwarz, K., van Den Broek, M., Kostka, S., Kraft, R., Soza, A., Schmidtke, G., Kloetzel, P.M. and Groettrup, M. (2000) Overexpression of the proteasome subunits LMP2, LMP7, and MECL-1, but not PA28 α/β, enhances the presentation of an immunodominant lymphocytic choriomeningitis virus T cell epitope. J. Immunol. 165, 768–778.
[35] Hallermalm, K., Seki, K., Wei, C., Castelli, C., Rivoltini, L., Kiessling, R. and Levitskaya, J. (2001) Tumor necrosis factor-α induces coordinated changes in major histocompatibility class I presentation pathway, resulting in increased stability of class I complexes at the cell surface. Blood 98, 1108–1115.
[36] Fujita, T., Reis, L.F., Watanabe, N., Kimura, Y., Taniguchi, T. and Vilcek, J. (1989) Induction of the transcription factor IRF-1 and interferon-β mRNAs by cytokines and activators of second-messenger pathways. Proc. Natl. Acad. Sci. USA 86, 9936–9940.
[37] Miyamoto, M., Fujita, T., Kimura, Y., Maruyama, M., Harada, H., Sudo, Y., Miyata, T. and Taniguchi, T. (1988) Regulated expression of a gene encoding a nuclear factor, IRF-1, that specifically binds to IFN-β gene regulatory elements. Cell 54, 903–913.

Regulation of murine chronic colitis by $CD4^+CD25^-$ programmed death-1^+ T cells

Teruji Totsuka[1], Takanori Kanai[1], Shin Makita[1], Rei Fujii[1], Yasuhiro Nemoto[1], Shigeru Oshima[1], Ryuichi Okamoto[1], Akemi Koyanagi[2], Hisaya Akiba[3], Ko Okumura[3], Hideo Yagita[3] and Mamoru Watanabe[1]

[1] Department of Gastroenterology and Hepatology, Graduate School, Tokyo Medical and Dental University, Tokyo, Japan
[2] Division of Cellular Biology, Juntendo University School of Medicine, Tokyo, Japan
[3] Department of Immunology, Juntendo University School of Medicine, Tokyo, Japan

Naturally arising $CD4^+CD25^+$ regulatory T (T_R) cells are engaged in the maintenance of self tolerance and prevention of autoimmune diseases. However, accumulating evidence suggests that a fraction of peripheral $CD4^+CD25^-$ T cells also possesses regulatory activity. Programmed death-1 (PD-1) is a new member of the CD28/CTLA-4 family, which has been implicated in the maintenance of peripheral self tolerance. Here, we identified a subpopulation of $CD4^+CD25^-PD\text{-}1^+$ T cells in the spleen of naive mice that constitutively expressed CTLA-4 and FoxP3 and was hypoproliferative in response to anti-CD3 antibody stimulation *in vitro*. However, the $CD4^+CD25^-PD\text{-}1^+$ T cells uniquely produced large amounts of IL-4 and IL-10 in response to anti-CD3 and anti-CD28 mAb stimulation, unlike the $CD4^+CD25^+$ T_R cells. The $CD4^+CD25^-PD\text{-}1^+$ T cells exhibited a suppressor activity against the proliferation of anti-CD3 antibody-stimulated $CD4^+CD25^-PD\text{-}1^-$ T cells *in vitro*, which was partially abrogated by anti-CTLA-4 mAb, but not by anti-IL-10 or anti-PD-1 mAb. Remarkably, the $CD4^+CD25^-PD\text{-}1^+$ T cells inhibited the development of colitis induced by adoptive transfer of $CD4^+CD45RB^{high}$ T cells into C.B17-scid/scid mice, albeit to a lesser extent than $CD4^+CD25^+$ T_R cells, in a CTLA-4-dependent manner. These results indicate that the $CD4^+CD25^-PD\text{-}1^+$ T cells contain substantial amounts of T_R cells that are involved in the maintenance of peripheral tolerance.

Received 16/3/04
Revised 16/3/05
Accepted 29/3/05

[DOI 10.1002/eji.200425109]

Key words: Regulatory T cells · Programmed death-1 · Colitis

Introduction

The intestinal mucosa harbors a large number of immune cells, which are constantly exposed to abundant exogenous stimuli such as bacterial flora and dietary antigens. To avoid an excessive inflammation that can damage the tissue, immune responses in the intestinal mucosa are finely controlled by a balance between pro-inflammatory helper/effector T cells and anti-inflammatory regulatory T (T_R) cells [1]. The pivotal role of T_R cells in preventing intestinal inflammation has been substantiated by the development of chronic colitis in C.B17-scid/scid mice after adoptive transfer of $CD4^+CD45RB^{high}$ T cells from normal BALB/c mice, which can be prevented by co-transfer of $CD4^+$

The first two authors contributed equally to this work.

Correspondence: Takanori Kanai, Department of Gastroenterology and Hepatology, Graduate School, Tokyo Medical and Dental University, 1-5-45 Yushima, Bunkyo-ku, Tokyo 113-8519, Japan
Fax: +81-3-5803-0268
e-mail: taka.gast@tmd.ac.jp

Abbreviations: **G3PDH:** Glyceraldehyde-3-phosphate dehydrogenase · **GITR:** Glucocorticoid-induced TNFR family-related protein · **LP:** Lamina propria · **MMC:** Mitomycin C · **PD-1:** Programmed death-1 · **SCID:** Severe combined immunodeficiency · **SD:** Standard deviation · **T_R:** Regulatory T · **Tr1:** T regulatory type 1

$CD45RB^{low}$ T cells containing T_R cells [2]. Recent studies have characterized several subsets of T_R cells, including IL-10-producing type-1 T_R (Tr1) cells [3], TGF-β-producing type-3 helper (Th3) cells [4], and naturally arising $CD4^+CD25^+$ T_R cells [5]. Among them, the $CD4^+CD25^+$ T_R cells are characterized by constitutive expression of the inhibitory receptor CTLA-4 [6, 7] and the forkhead/winged helix transcription factor FoxP3 [8], and mainly constitute the $CD4^+CD45RB^{low}$ T_R cells that prevent colitis [6]. Interestingly, CTLA-4 in these cells plays a critical functional role in their suppressor activity, since the blockade of CTLA-4 abolishes the ability of $CD4^+CD25^+$ T_R cells to prevent colitis [6].

Programmed death-1 (PD-1) is a new member of the CD28/CTLA-4 family of T cell costimulatory/inhibitory molecules [9]. PD-1 is expressed on activated T cells and down-regulates further T cell activation [10], like CTLA-4. Importantly, PD-1-deficient mice spontaneously develop autoimmune diseases [11, 12], suggesting an important role for PD-1 in the maintenance of self tolerance [13].

In the present study, we identified a subpopulation of $CD4^+CD25^-$ T cells expressing PD-1 in the spleen of naive mice, which also expressed CTLA-4 and FoxP3. These cells exhibited suppressor activity *in vitro* and prevented the $CD4^+CD45RB^{high}$ T cell-induced colitis. We also examined the functional involvement of CTLA-4 and PD-1 in this suppressor activity.

Results

Splenic $CD4^+$ T cells from naive mice contain $CD25^+PD\text{-}1^-$, $CD25^-PD\text{-}1^+$ and $CD25^+PD\text{-}1^+$ subpopulations

In addition to the $CD4^+CD25^+$ T_R cell population, accumulating evidence has shown that some $CD4^+CD25^-$ T cell subpopulations also exhibit regulatory activity [14–18]. Recent findings that (i) the $CD4^+CD25^+$ T_R cells constitutively express CTLA-4, (ii) PD-1 is a functional homologue of CTLA-4, and (iii) PD-1-deficient mice spontaneously develop autoimmune diseases prompted us to examine the expression and function of PD-1 on splenic $CD4^+$ T cells from naive BALB/c mice. As shown in Fig. 1A, PD-1 was expressed on a small fraction of $CD4^+$ T cells (7.7±0.8%), as was CD25 (7.8±0.7%). Three-color flow cytometry showed that $CD4^+$ T cells consisted of four fractions: $CD25^-PD\text{-}1^-$ (87.9±0.9%), $CD25^-PD\text{-}1^+$ (5.1±1.4%), $CD25^+PD\text{-}1^-$ (4.3±0.7%), and $CD25^+PD\text{-}1^+$ (3.0±0.4%) (Fig. 1B). In addition to CD25, $CD4^+$ T_R cells have been characterized by their expression of CTLA-4 [6, 7], CD45RB [2], integrin $\alpha_E\beta_7$ [16], and glucocorticoid-induced TNFR family-

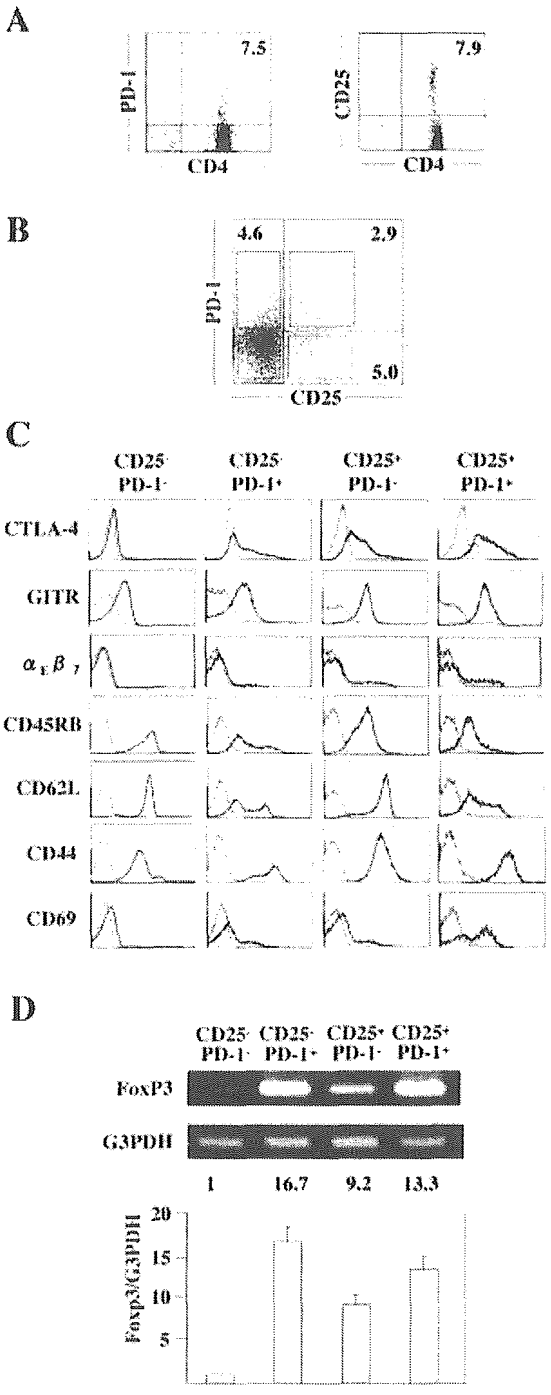

Fig. 1. Phenotypic characterization of splenic $CD4^+$ T cells expressing CD25 and/or PD-1. (A) FACS analysis shows the expression of PD-1 or CD25 on a minor population of splenic $CD4^+$ T cells (7.7±0.8% $PD\text{-}1^+$ and 7.8±0.7% $CD25^+$; means ± SD from six independent experiments). (B) Correlation of CD25 and PD-1 expression on splenic $CD4^+$ T cells. (C) Expression of various markers in $CD25^-PD\text{-}1^-$, $CD25^-PD\text{-}1^+$, $CD25^+PD\text{-}1^-$, and $CD25^+PD\text{-}1^+$ subpopulations of splenic $CD4^+$ T cells. Thick histograms represent staining with mAb against the indicated markers. Thin histograms represent staining with isotype-matched control IgG. (D) Expression of FoxP3 mRNA was determined by RT-PCR. Samples were normalized to 18S rRNA, and a relative value of 1.0 was given to the FoxP3/G3PDH ratio of $CD4^+CD25^-PD\text{-}1^-$ cells. Data represent the means ± SEM of three independent experiments.

related protein (GITR) [19]. As reported previously, $CD4^+CD25^+$ T cells expressed CTLA-4 at a high level, irrespective of PD-1 expression (Fig. 1C). Interestingly, $CD4^+CD25^-PD\text{-}1^+$ T cells also expressed CTLA-4 at a moderate level, while $CD4^+CD25^-PD\text{-}1^-$ T cells did not. GITR was expressed at a high level on both $CD4^+CD25^+PD\text{-}1^-$ and $CD4^+CD25^+PD\text{-}1^+$ cells, but at a moderate level on both $CD4^+CD25^-PD\text{-}1^-$ and $CD4^+CD25^-PD\text{-}1^+$ cells (Fig. 1C). Integrin $\alpha_E\beta_7$ was expressed on substantial parts of $CD4^+CD25^+PD\text{-}1^{+/-}$ cells and a marginal part of $CD4^+CD25^-PD\text{-}1^+$ cells, but not on $CD4^+CD25^-PD\text{-}1^-$ cells (Fig. 1C). CD45RB was expressed at low levels on both $CD4^+CD25^+PD\text{-}1^-$ and $CD4^+CD25^+PD\text{-}1^+$ cells, but at a high level on $CD4^+CD25^-PD\text{-}1^-$ cells. $CD4^+CD25^-PD\text{-}1^+$ cells showed a heterogeneous profile, mainly $CD45RB^{low}$ (Fig. 1C). We also examined the expression of naive/memory markers (CD62L and CD44) and an activation marker (CD69) on these subpopulations (Fig. 1C). While $CD4^+CD25^-PD\text{-}1^-$ cells mostly showed a $CD62L^{high}$ $CD44^{low}$ naive phenotype, the $CD4^+CD25^-PD\text{-}1^+$ population contained substantial amounts of $CD62L^{low}CD44^{high}$ memory cells. It was also notable that the $CD4^+CD25^+PD\text{-}1^+$ population was mainly composed of $CD62L^{low}CD44^{high}$ memory cells and also contained recently activated $CD69^+$ cells, while the $CD4^+CD25^+PD\text{-}1^-$ population was mostly composed of $CD62L^{high}CD44^{intermediate}$ cells (Fig. 1C). Furthermore, both $CD4^+CD25^+PD\text{-}1^-$ and $CD4^+CD25^+PD\text{-}1^+$ cells expressed FoxP3 mRNA at high levels (Fig. 1D). Notably, $CD4^+CD25^-PD\text{-}1^+$ cells also expressed FoxP3 at a high level, while $CD4^+CD25^-PD\text{-}1^-$ cells did not.

Functional characterization of $CD4^+CD25^-PD\text{-}1^+$, $CD4^+CD25^+PD\text{-}1^-$, and $CD4^+CD25^+PD\text{-}1^+$ populations *in vitro*

To characterize their functions *in vitro*, we isolated the $CD25^-PD\text{-}1^-$, $CD25^-PD\text{-}1^+$, $CD25^+PD\text{-}1^-$, and $CD25^+PD\text{-}1^+$ populations from splenic $CD4^+$ T cells by FACS sorting (Fig. 2A). A non-blocking anti-PD-1 mAb (RMP1–30) was used to avoid a possible interruption of PD-1 function. As previously reported on the whole $CD4^+CD25^+$ population [5], both $CD4^+CD25^+PD\text{-}1^-$ and $CD4^+CD25^+PD\text{-}1^+$ cells were anergic and did not proliferate in response to anti-CD3 antibody stimulation in the presence of $CD4^-$ splenocytes as APC (Fig. 2B). Notably, $CD4^+CD25^-PD\text{-}1^+$ cells were also markedly hypoproliferative, while $CD4^+CD25^-PD\text{-}1^-$ cells proliferated vigorously. When co-cultured with the $CD4^+CD25^-PD\text{-}1^-$ responder cells, both $CD4^+CD25^+PD\text{-}1^-$ and $CD4^+CD25^+PD\text{-}1^+$ cells suppressed their proliferation with a similar potency (Fig. 2C). $CD4^+CD25^-PD\text{-}1^+$ cells, but not $CD4^+CD25^-PD\text{-}1^-$ cells, also significantly suppressed the proliferation, albeit with a lesser potency. When stimulated with anti-CD3 and anti-CD28 mAb, only the $CD4^+CD25^-PD\text{-}1^-$ population produced large amounts of IFN-γ and IL-2 (Fig. 2D). Notably, the $CD4^+CD25^-PD\text{-}1^+$ population produced distinctively large amounts of IL-4 and IL-10. To determine whether IL-4 and IL-10 were produced by the same cells or by two distinct subpopulations of $CD4^+CD25^-PD\text{-}1^+$ cells, we next examined intracellular IL-4 and IL-10 by flow cytometry. As shown in Fig. 2E and F, the $CD25^-PD\text{-}1^+$ population uniquely contained substantial frequencies of cells producing either IL-4 or IL-10, but few cells producing both IL-4 and IL-10, indicating that the $CD4^+CD25^-PD\text{-}1^+$ population is as heterogeneous as the classical $CD4^+CD25^+$ T_R cells.

Correlation of the $CD4^+CD25^-PD\text{-}1^+$ T_R population with the $CD4^+CD45RB^{low}$ T_R population

We next examined the correlation of the $CD4^+CD25^-PD\text{-}1^+$ T_R population with the known $CD4^+CD45RB^{low}$ T_R population [2]. As shown in Fig. 3A, the $CD4^+CD45RB^{low}$ population contained $CD25^+PD\text{-}1^{+/-}$ cells (7.9±1.2%) and $CD25^-PD\text{-}1^+$ cells (4.6±0.9%). We then isolated $CD25^+$, $CD25^-PD\text{-}1^+$, and $CD25^-PD\text{-}1^-$ subpopulations from $CD4^+CD45RB^{low}$ cells by FACS sorting (Fig. 3B). FoxP3 was expressed in the $CD25^-PD\text{-}1^+$ cells and the $CD25^+$ cells, but not in the $CD25^-PD\text{-}1^-$ cells (Fig. 3C). The $CD25^-PD\text{-}1^+$ cells exhibited a significant T_R activity in the *in vitro* suppression assay, albeit less potently than the $CD25^+$ cells (Fig. 3D). These results indicate that $CD25^-PD\text{-}1^+$ T_R cells constitute a substantial part of the $CD4^+CD45RB^{low}$ T_R cells.

Correlation of the $CD4^+CD25^-PD\text{-}1^+$ T_R population with the $CD4^+CD25^-GITR^+$ T_R population

Since we have previously identified a new $CD4^+CD25^-$ T_R population expressing GITR [18], we next examined the correlation of the $CD4^+CD25^-PD\text{-}1^+$ T_R population with the $CD4^+CD25^-GITR^+$ T_R population. As shown in Fig. 4A, $CD4^+CD25^-$ cells contained $PD\text{-}1^-GITR^+$ cells (5.3±1.1%), $PD\text{-}1^+GITR^-$ cells (3.1±0.8%), and $PD\text{-}1^+GITR^+$ cells (1.2±0.4%). We isolated $CD25^+$, $CD25^-PD\text{-}1^+GITR^-$, and $CD25^-PD\text{-}1^+GITR^+$ cells by FACS sorting (Fig. 4B). In the *in vitro* suppression assay, the $PD\text{-}1^+$ subpopulations exhibited significant T_R activities, regardless of GITR expression, albeit less potently than the $CD25^+$ cells (Fig. 4C). These results indicate that $CD25^-PD\text{-}1^+$ T cells constitute a minor part of the $CD25^-GITR^+$ T_R cells, but there is also a substantial $CD25^-GITR^-PD\text{-}1^+$ T_R population.

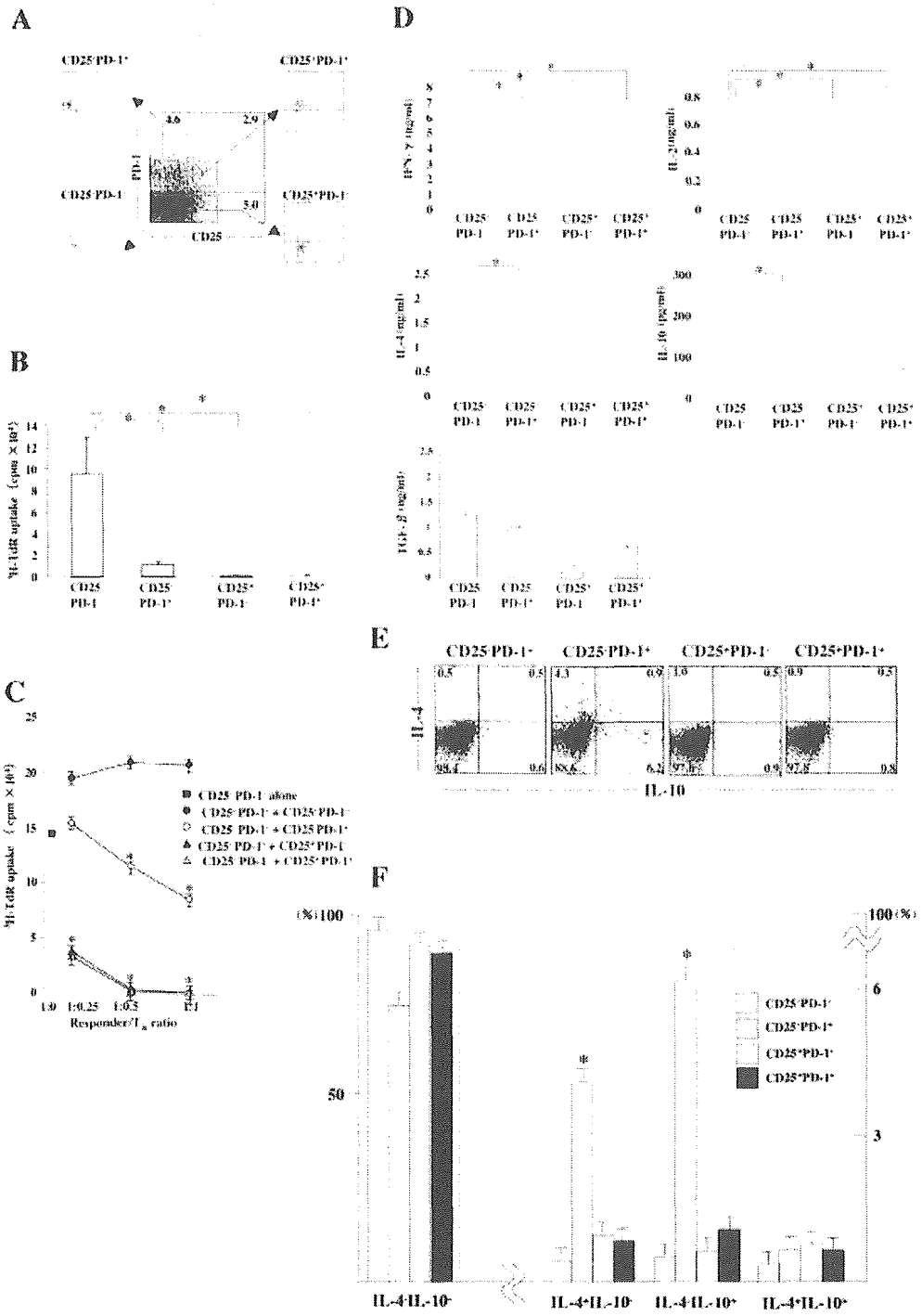

Fig. 2. Functional characterization of $CD25^-PD\text{-}1^+$ subpopulation of splenic $CD4^+$ T cells *in vitro*. (A) $CD25^-PD\text{-}1^-$, $CD25^-PD\text{-}1^+$, $CD25^+PD\text{-}1^-$, and $CD25^+PD\text{-}1^+$ populations were isolated from MACS-purified splenic $CD4^+$ T cells by FACS sorting. Typical profiles of the sorted fractions are shown. (B) Proliferative response. Cells were stimulated with 1 μg/ml anti-CD3 mAb in the presence of MMC-treated $CD4^-$ splenocytes as APC for 72 h. [^{3}H]thymidine (^{3}H-TdR) uptake was determined for the last 9 h. Data are represented as the means ± SD of triplicate samples; $^*p<0.05$. (C) Suppressive activity. The suppressive activity of the indicated subpopulations was determined by co-culturing with $CD4^+CD25^-PD\text{-}1^-$ responder cells at the different responder/T_R ratios in the presence of anti-CD3 mAb and APC for 72 h. As a negative control, $CD4^+CD25^-PD\text{-}1^-$ cells were also included. [^{3}H]thymidine (^{3}H-TdR) uptake was determined for the last 9 h. Data are represented as the means ± SD of triplicate samples. $^*p<0.05$ compared to responder cells alone. (D) Cytokine production. Cells were stimulated with plate-bound anti-CD3 mAb and soluble anti-CD28 mAb for 72 h. Cytokines in the supernatants were measured by ELISA. Data are represented as the means ± SD of triplicate samples; $^*p<0.05$. (E) Intracellular cytokine staining. Each population was stained with PE-conjugated anti-IL-4 mAb and FITC-conjugated anti-IL-10 mAb and analyzed for intracellular IL-4 and IL-10 by flow cytometry. Representative FACS plots show the expression of IL-4 and IL-10. (F) The frequencies of IL-4- and/or IL-10-producing cells were analyzed in the indicated subpopulations by flow cytometry. Data are represented as the means ± SD of three independent experiments.

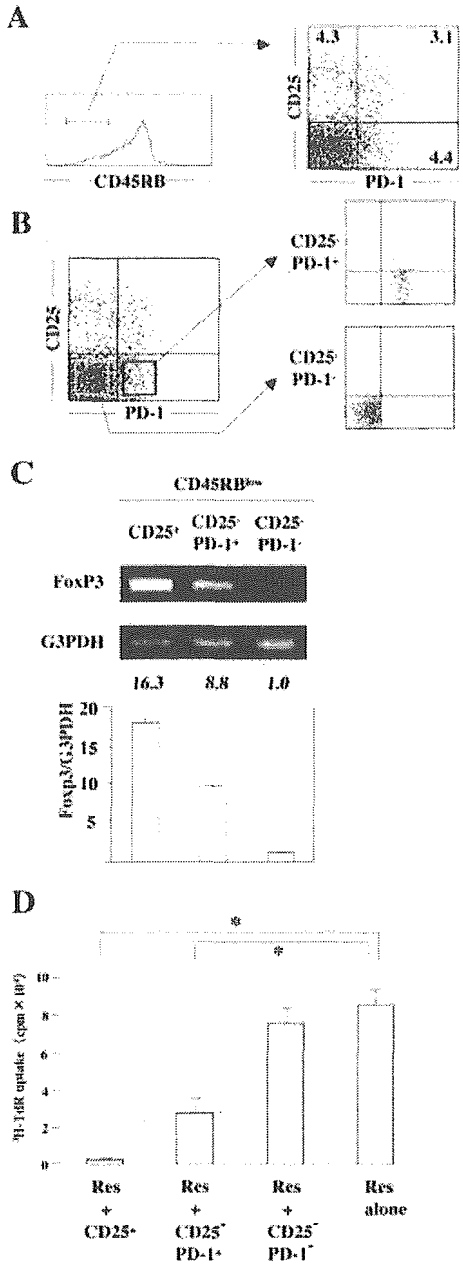

Fig. 3. Characterization of $CD25^+$, $CD25^-PD\text{-}1^+$, and $CD25^-PD\text{-}1^-$ subpopulations in splenic $CD4^+CD45RB^{low}$ T cells. (A) PD-1/CD25 expression on $CD4^+CD45RB^{low}$ T cells. (B) $CD25^-PD\text{-}1^+$ and $CD25^-PD\text{-}1^-$ subpopulations in $CD4^+CD45RB^{low}$ T cells were sorted on a FACS Vantage. (C) Expression of FoxP3 mRNA in the indicated subpopulations was determined by RT-PCR as described in Fig. 1D. (D) Suppressive activity of the indicated subpopulations was determined as described in Fig. 2C, at a responder (Res)/T_R ratio of 1:1. $^*p<0.05$.

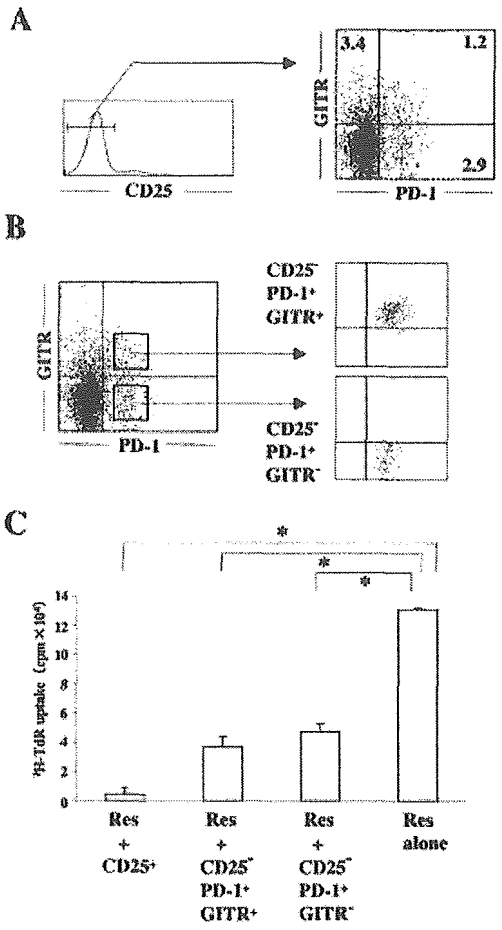

Fig. 4. Characterization of $GITR^+PD\text{-}1^+$ and $GITR^-PD\text{-}1^+$ subpopulations in splenic $CD4^+CD25^-$ T cells. (A) Correlation of GITR and PD-1 expression on $CD4^+CD25^-$ cells. (B) $GITR^+PD\text{-}1^+$ and $GITR^-PD\text{-}1^+$ subpopulations were sorted on a FACS Vantage. Each population was >98.0% pure upon reanalysis. (C) Suppressive activity of the indicated subpopulations was determined as described in Fig. 3D. $^*p<0.05$.

Functional contribution of CTLA-4, but not PD-1 or IL-10, to suppressor activity of $CD4^+CD25^-PD\text{-}1^+$ T_R cells *in vitro*

The data showing that $CD4^+CD25^-PD\text{-}1^+$ T_R cells produced large amount of IL-4 and IL-10 and expressed CTLA-4 and PD-1 raised the possibility that these cytokines and costimulatory molecules might mediate the suppressor activity of these cells. To address this possibility, we blocked IL-4 and IL-10 in an *in vitro* suppression assay. Addition of a neutralizing mAb against IL-10 had no effect on the suppression of proliferation by $CD4^+CD25^-PD\text{-}1^+$, $CD4^+CD25^+PD\text{-}1^-$, and $CD4^+CD25^+PD\text{-}1^+$ cells (Fig. 5A). In contrast, a neutralizing mAb against IL-4 partially inhibited proliferation of the $CD4^+CD25^-PD\text{-}1^-$ responder T cells and mostly abolished the residual proliferation in the presence of $CD4^+CD25^-PD\text{-}1^+$ T_R cells. Interestingly, addition of a blocking anti-CTLA-4 mAb partially but significantly abolished the suppression by $CD4^+CD25^-PD\text{-}1^+$ T_R cells, but not that by $CD4^+CD25^+PD\text{-}1^{+/-}$ T_R cells (Fig. 5B). In contrast, either a blocking anti-PD-1 mAb (RMP1–14) or a non-blocking anti-PD-1 mAb (RMP1–30) did not affect the suppression by all three T_R subsets (Fig. 5B).

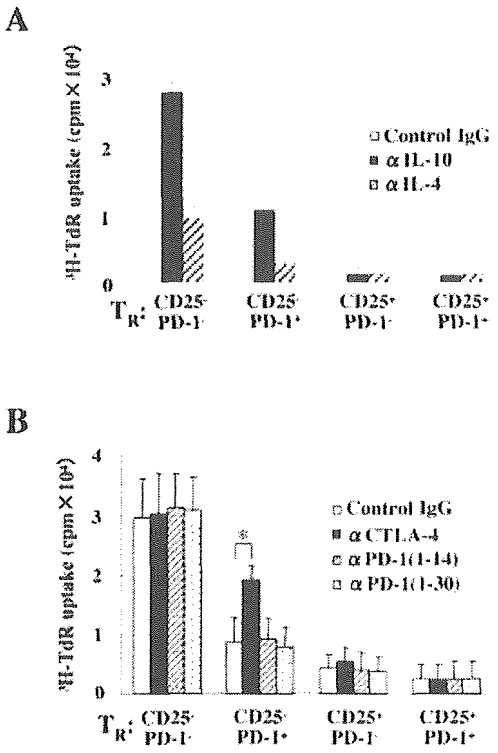

Fig. 5. Effect of anti-IL-10, anti-IL-4, anti-CTLA-4, or anti-PD-1 mAb on the suppressor activity of $CD25^-PD\text{-}1^+$, $CD25^+PD\text{-}1^-$, and $CD25^+PD\text{-}1^+$ regulatory $CD4^+$ T cell subpopulations *in vitro*. $CD4^+CD25^-PD\text{-}1^-$ T cells (responder) were co-cultured with the indicated subpopulations of T_R cells at a 1:1 ratio in the presence of anti-CD3 mAb and MMC-treated $CD4^-$ splenocytes as APC. Control IgG, anti-IL-10 or anti-IL-4 mAb (A), and anti-CTLA-4 or anti-PD-1 mAb (B) were added at the start of the culture. [^{3}H]thymidine (^{3}H-TdR) uptake was determined for the last 9 h of a 72-h culture. Data are represented as the means ± SD of triplicate samples; $^*p<0.05$.

T_R function of $CD4^+CD25^-PD\text{-}1^+$ cells in murine chronic colitis model

We next investigated the suppressor activity of $CD4^+CD25^-PD\text{-}1^+$ and $CD4^+CD25^+PD\text{-}1^{+/-}$ T_R cells in a murine colitis model induced by adoptive transfer of $CD4^+CD45RB^{high}$ T cells into severe combined immunodeficiency (SCID) mice [2]. As illustrated in Fig. 6A, SCID mice were injected with $CD4^+CD45RB^{high}$ T cells with or without $CD4^+CD25^-PD\text{-}1^+$, $CD4^+CD25^+PD\text{-}1^-$, or $CD4^+CD25^+PD\text{-}1^+$ T_R cells. As previously reported with the whole $CD4^+CD25^+$ T_R population [6], the co-transfer of either $CD4^+CD25^+PD\text{-}1^-$ or $CD4^+CD25^+PD\text{-}1^+$ cells potently ameliorated the $CD4^+CD45RB^{high}$ T cell-induced colitis, as estimated by wasting (Fig. 6B) and clinical score (Fig. 6C). $CD4^+CD25^-PD\text{-}1^+$ cells also significantly ameliorated the disease, albeit to a lesser extent than $CD4^+CD25^+PD\text{-}1^{+/-}$ cells. Histological examination showed prominent epithelial hyperplasia with glandular elongation, with a massive infiltration of mononuclear cells in the lamina propria (LP) of the colon of mice transferred with $CD4^+CD45RB^{high}$ T cells alone (Fig. 6D). In contrast, the glandular elongation was mostly abrogated and only few mononuclear cells were observed in the LP of the colon of mice co-transferred with $CD4^+CD25^-PD\text{-}1^+$, $CD4^+CD25^+PD\text{-}1^-$, or $CD4^+CD25^+PD\text{-}1^+$ cells (Fig. 6D). The differences were statistically significant as estimated by histological scoring (Fig. 6E). At 7 weeks after T cell transfer, all mice were sacrificed and $CD4^+$ T cells were collected from spleen and colon. As shown in Fig. 6F, co-transfer of $CD4^+CD25^-PD\text{-}1^+$ cells inhibited the expansion and/or infiltration of $CD4^+CD45RB^{high}$ T cells as potently as $CD4^+CD25^+PD\text{-}1^{+/-}$ cells.

To determine the effect on Th1/Th2 development, we measured IFN-γ, IL-2, IL-4, and IL-10 production by anti-CD3/CD28 mAb-stimulated $CD4^+$ LP T cells. As shown in Fig. 6G, production of Th1 cytokines (IFN-γ and IL-2) was significantly reduced by co-transfer of $CD4^+CD25^-$ $PD\text{-}1^+$, $CD4^+CD25^+PD\text{-}1^-$, or $CD4^+$ $CD25^+PD\text{-}1^+$ cells. In contrast, production of Th2 cytokines (IL-4 and IL-10) was not significantly affected by these populations.

Suppression of colitis is restricted to a subpopulation of $CD4^+CD45RB^{low}PD\text{-}1^+$ but not $CD4^+CD45RB^{low}PD\text{-}1^-$ cells in $CD25^-$ T_R cells

We further assessed whether *in vivo* suppression of colitis is restricted to a subpopulation of $CD4^+$ $CD45RB^{low}PD\text{-}1^+$ but not $CD4^+CD45RB^{low}PD\text{-}1^-$ cells in the $CD25^-$ T_R cells. To this end, we isolated $CD25^+$, $CD25^-PD\text{-}1^+$, and $CD25^-PD\text{-}1^-$ subpopulations from $CD4^+CD45RB^{low}$ cells by FACS sorting (Fig. 7A); thereafter, we co-injected $CD4^+CD45RB^{low}CD25^-PD\text{-}1^-$, $CD4^+CD45RB^{low}CD25^-PD\text{-}1^+$, or $CD4^+CD45RB^{low}$ $CD25^+$ T cells together with $CD4^+CD45RB^{high}$ cells into SCID mice (Fig. 7A). The co-transfer of $CD4^+CD45RB^{low}$ $CD25^-PD\text{-}1^+$ or $CD4^+CD45RB^{low}CD25^+$ cells, but not $CD4^+CD45RB^{low}CD25^-PD\text{-}1^-$ cells, significantly suppressed the $CD4^+CD45RB^{high}$ T cell-induced colitis, as estimated by wasting (Fig. 7B) and clinical score (Fig. 7C). Histological examination showed that the colitis was mostly abrogated in mice co-transferred with $CD4^+CD45RB^{low}CD25^-PD\text{-}1^+$ or $CD4^+CD45RB^{low}$ $CD25^+$ but not $CD4^+CD45RB^{low}CD25^-PD\text{-}1^-$ T cells (Fig. 7D). The differences were statistically significant as estimated by histological scoring (Fig. 7E). As shown in Fig. 7F and G, the co-transfer of $CD4^+CD45RB^{low}$ $CD25^-PD\text{-}1^+$ cells inhibited the expansion and/or infiltration of $CD4^+CD45RB^{high}$ T cells at 6 weeks after the transfer as potently as $CD4^+CD45RB^{low}CD25^+$ T_R cells.

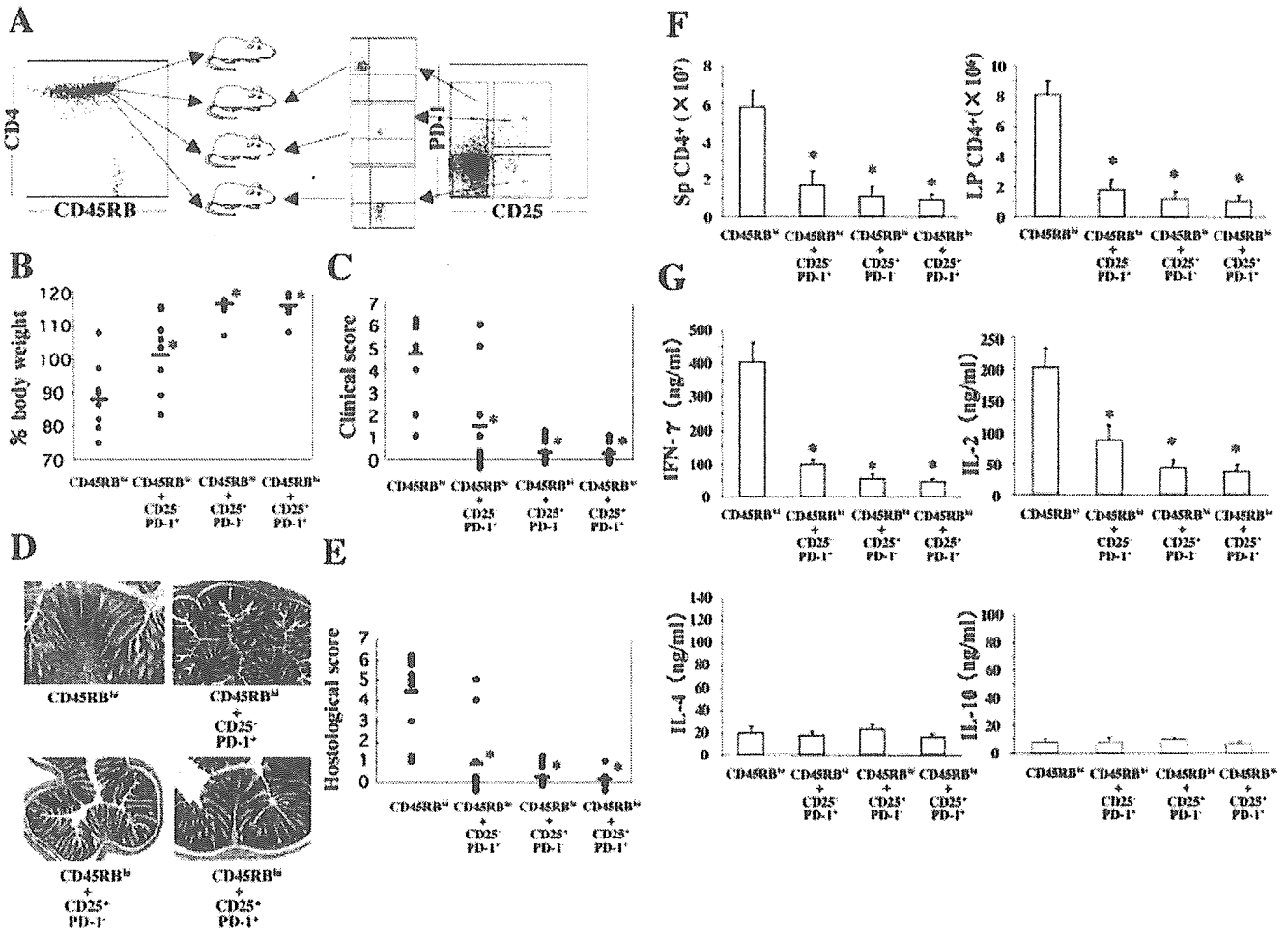

Fig. 6. $CD4^+CD25^-PD\text{-}1^+$ T_R cells, as well as $CD4^+CD25^+PD\text{-}1^-$ and $CD4^+CD25^+PD\text{-}1^+$ T_R cells, inhibit the development of colitis induced by adoptive transfer of $CD4^+CD45RB^{high}$ T cells into SCID mice. (A) Ten SCID mice in each group were injected i.p. with the following T cell subpopulations: (1) $CD4^+CD45RB^{high}$ alone (3×10^5 cells); (2) $CD4^+CD45RB^{high}$ (3×10^5 cells) + $CD4^+CD25^-PD\text{-}1^+$ (1×10^5 cells); (3) $CD4^+CD45RB^{high}$ (3×10^5 cells) + $CD4^+CD25^+PD\text{-}1^-$ (1×10^5 cells); or (4) $CD4^+CD45RB^{high}$ (3×10^5 cells) + $CD4^+CD25^+PD\text{-}1^+$ (1×10^5 cells). (B) Body weight at 7 weeks after transfer. *, $p<0.05$ compared to $CD45RB^{high}$ alone. (C) Clinical score at 7 weeks after transfer. *, $p<0.05$ compared to $CD45RB^{high}$ alone. (D) Histopathology of the distal colon at 7 weeks after transfer. Original magnification, ×100. (E) Histological score at 7 weeks after transfer. *, $p<0.05$ compared to $CD45RB^{high}$ alone. (F) Number of $CD4^+$ T cells in the spleen (Sp) and LP at 7 weeks after transfer. Data are indicated as the means ± SD of seven mice in each group. *, $p<0.05$ compared to $CD45RB^{high}$ alone. (G) Cytokine production by LP $CD4^+$ T cells. LP $CD4^+$ T cells were stimulated with plate-bound anti-CD3 mAb and soluble anti-CD28 mAb for 72 h. Cytokines in the supernatants were measured by ELISA. Data are indicated as the means ± SD of seven mice in each group. *, $p<0.05$ compared to $CD45RB^{high}$ alone.

Critical contribution of CTLA-4 but not PD-1 to suppressor activity of $CD4^+CD25^-PD\text{-}1^+$ T_R cells *in vivo*

It has been reported that CTLA-4 is functionally involved in the suppression of $CD4^+CD45RB^{high}$ T cell-induced colitis by $CD4^+CD25^+$ T_R cells [6]. Given the expression of CTLA-4 and PD-1 on $CD4^+CD25^-PD\text{-}1^+$ T_R cells, we finally examined the functional contribution of CTLA-4 and PD-1 to their suppressor activity *in vivo*. As illustrated in Fig. 8A, $CD4^+CD45RB^{high}$ T cells and $CD4^+CD25^-PD\text{-}1^+$ T_R cells were co-transferred into SCID mice, and a blocking anti-CTLA-4 mAb, a blocking anti-PD-1 mAb (RMP1–14), or a non-blocking anti-PD-1 mAb (RMP1–30) was administrated from the day of T cell transfer for 6 weeks. Remarkably, anti-CTLA-4 mAb but neither anti-PD-1 mAb totally abrogated the ameliorating effect of $CD4^+CD25^-PD\text{-}1^+$ T_R cells on wasting (Fig. 8B), clinical score (Fig. 8C), histopathology (Fig. 8D, E), and $CD4^+$ T cell expansion/infiltration (Fig. 8F). These results suggested that CTLA-4, but not PD-1, was functionally involved in the suppression of colitis by $CD4^+CD25^-PD\text{-}1^+$ T_R cells.

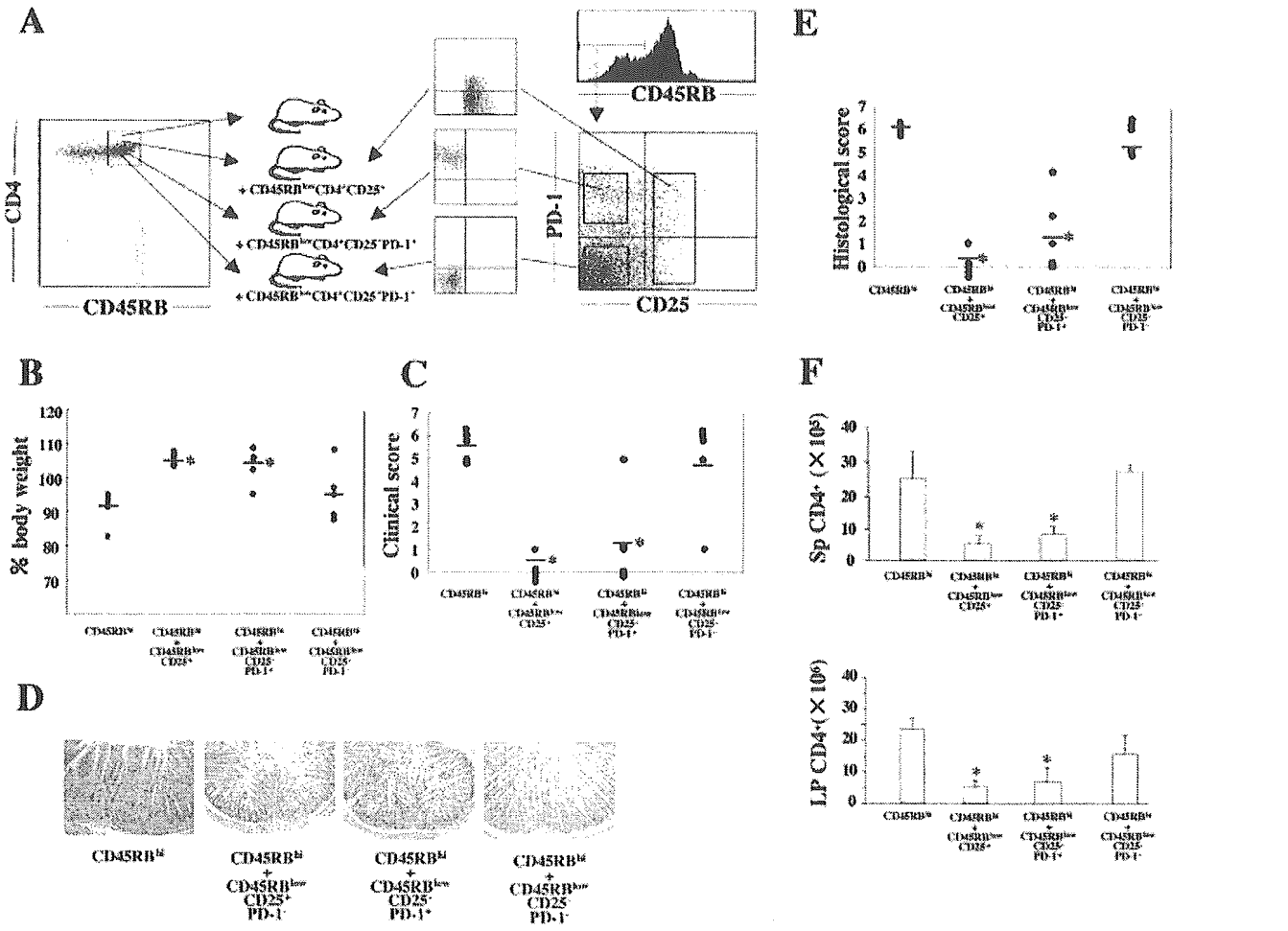

Fig. 7. $CD4^+CD45RB^{low}CD25^-PD\text{-}1^+$ T_R cells inhibit the development of colitis induced by adoptive transfer of $CD4^+CD45RB^{high}$ T cells into SCID mice. (A) Five SCID mice in each group were injected i.p. with the following T cell subpopulations: (1) $CD4^+CD45RB^{high}$ alone (3×10^5 cells); (2) $CD4^+CD45RB^{high}$ (3×10^5 cells) + $CD4^+CD45RB^{low}CD25^+$ (1×10^5 cells); (3) $CD4^+CD45RB^{high}$ (3×10^5 cells) + $CD4^+CD45RB^{low}CD25^-PD\text{-}1^+$ (1×10^5 cells); or (4) $CD4^+CD45RB^{high}$ (3×10^5 cells) + $CD4^+CD45RB^{low}CD25^-PD\text{-}1^-$ (1×10^5 cells). (B) Body weight at 7 weeks after transfer. *, $p<0.05$ compared to $CD45RB^{high}$ alone. (C) Clinical score at 7 weeks after transfer. *, $p<0.05$ compared to $CD45RB^{high}$ alone. (D) Histopathology of the distal colon at 7 weeks after transfer. Original magnification, ×100. (E) Histological score at 7 weeks after transfer. *, $p<0.05$ compared to $CD45RB^{high}$ alone. (F) Number of $CD4^+$

Discussion

In the present study, we first determined the expression of PD-1 on splenic $CD4^+$ T cells from naive mice (Fig. 1). PD-1 was expressed on a minor population of $CD4^+CD25^-$ T cells and on about half of the $CD4^+CD25^+$ T cells. Among the $CD4^+CD25^-$ T cells, the majority of $PD\text{-}1^+$ cells were characterized by an effector/memory-like phenotype ($CD45RB^{low}CD62L^{low}CD44^{high}$) and constitutively expressed CTLA-4, while the $PD\text{-}1^-$ cells showed a naive phenotype ($CD45RB^{high}CD62L^{high}CD44^{low}$) and did not express CTLA-4. Among the $CD4^+CD25^+$ T cells, the $PD\text{-}1^+$ cells were also characterized by the effector/memory-like phenotype ($CD45RB^{low}CD62L^{low}CD44^{high}$), while the $PD\text{-}1^-$ cells showed a naive-like phenotype ($CD45RB^{intermediate}CD62L^{high}CD44^{intermediate}$). These results suggest that PD-1 expression can be used to discriminate subpopulations of both $CD4^+CD25^-$ and $CD4^+CD25^+$ T cells, possibly at distinct differentiation stages. Since PD-1 is expressed on T cells upon activation [10], the PD-1 expression may reflect a continuous activation of these cells *in vivo* by endogenous stimuli such as self antigens and bacterial flora.

Recent studies have revealed that FoxP3 is a master regulator of the development and function of $CD4^+CD25^+$ T_R cells [8]. The $CD4^+CD25^-PD\text{-}1^+$ cells also expressed FoxP3 (Fig. 1D), which might be responsible for the CTLA-4 expression, hypoproliferation, and suppressor activity of these cells. It has been

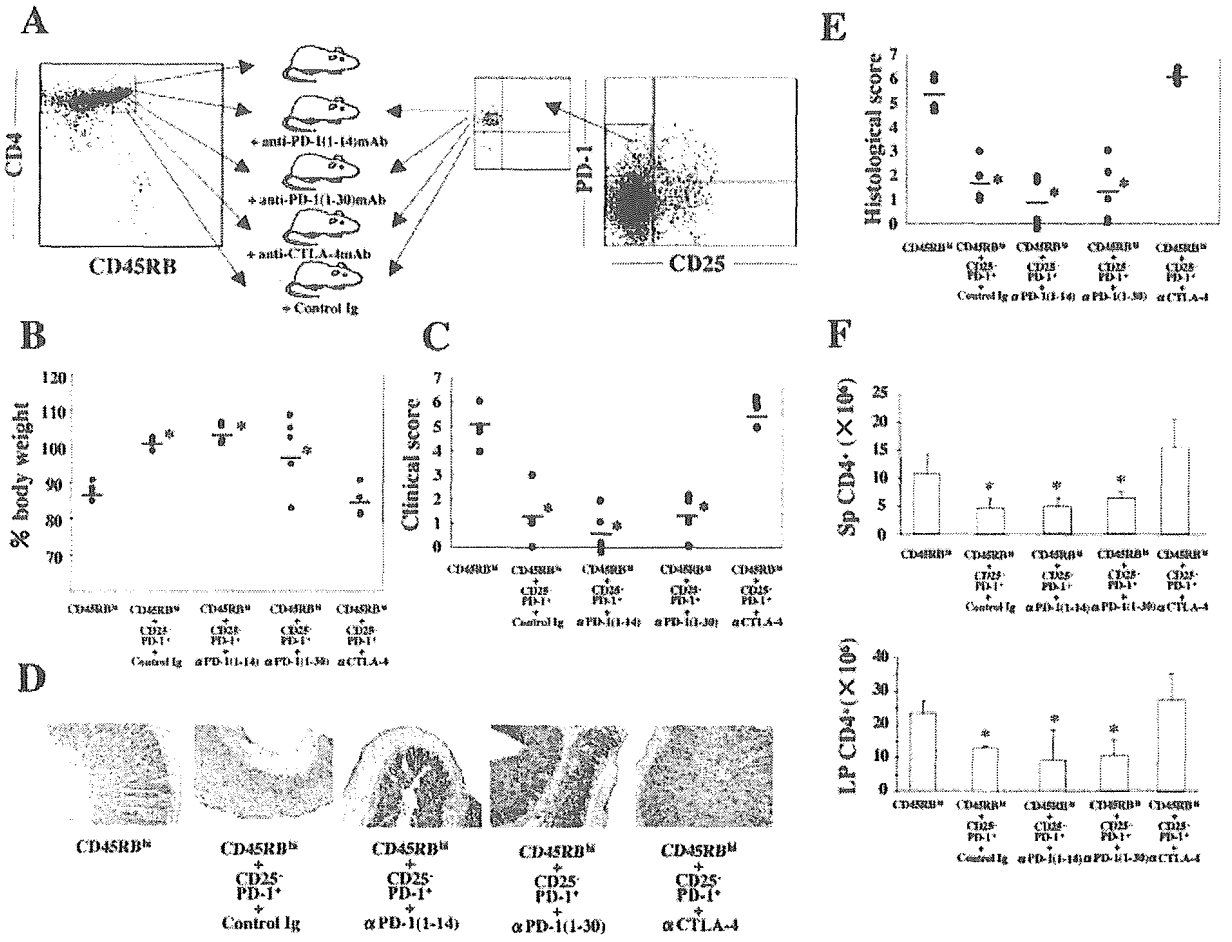

Fig. 8. Critical contribution of CTLA-4 but not PD-1 to the suppressor activity of $CD4^+CD25^-PD\text{-}1^+$ T_R cells *in vivo*. (A) Five SCID mice in each group were injected i.p. with $CD4^+CD45RB^{high}$ cells (3×10^5) alone or $CD4^+CD45RB^{high}$ (3×10^5) + $CD4^+CD25^-PD\text{-}1^+$ (1×10^5) cells. Some groups of mice were given 200 μg control IgG, blocking anti-PD-1 mAb (RMP1–14), non-blocking anti-PD-1 mAb (RMP1–30), or anti-CTLA-4 mAb, three times per week for 6 weeks from the day of T cell transfer. (B) Body weight at 7 weeks after transfer. *, $p<0.05$ compared to $CD45RB^{high}$ alone. (C) Clinical score at 7 weeks after transfer. *, $p<0.05$ compared to $CD45RB^{high}$ alone. (D) Histopathology of the distal colon at 7 weeks after transfer. Original magnification, ×100. (E) Histological score at 7 weeks after transfer. *, $p<0.05$ compared to $CD45RB^{high}$ alone. (F) Number of $CD4^+$ T cells in the spleen (Sp) and LP at 7 weeks after transfer. Data are indicated as the means ± SD of five mice in each group. *, $p<0.05$ compared to $CD45RB^{high}$ alone.

demonstrated that the $CD4^+CD25^+$ T_R cells expressing FoxP3 develop in the thymus [8]. However, recent papers have shown that FoxP3 can be induced in peripheral $CD4^+CD25^-$ T cells by *in vitro* stimulation [20, 21]. It remains to be determined whether the $CD4^+CD25^-PD\text{-}1^+$ T cells expressing FoxP3 develop in the thymus or in the periphery.

The *in vitro* studies showed a unique functional property of the $CD4^+CD25^-PD\text{-}1^+$ T cells. They were hypoproliferative in response to anti-CD3 antibody stimulation, like the $CD4^+CD25^+$ T_R cells (Fig. 2B), and suppressed the proliferative response of $CD4^+CD25^-PD\text{-}1^-$ responder cells, albeit less potently than the classical $CD4^+CD25^+$ T_R cells (Fig. 2C). Of note, the $CD4^+CD25^-PD\text{-}1^+$ cells produced distinctively large amounts of IL-4 and IL-10 in response to anti-CD3/CD28 mAb stimulation (Fig. 2D), suggesting Th2 or Tr1-like properties. Intracellular staining revealed that the $CD4^+CD25^-PD\text{-}1^+$ cells contained Th2-like cells producing IL-4 but not IL-10 and Tr1-like cells producing IL-10 but not IL-4 (Fig. 2E). These two populations may represent Th2 and Tr1 cells developed in response to some endogenous stimulus, such as a self antigens and bacterial flora. The IL-4 produced by $CD4^+CD25^-PD\text{-}1^+$ cells appeared to be responsible for the limited ability of these cells to suppress the proliferation of $CD4^+CD25^-PD\text{-}1^-$ cells (Fig. 2C), since the residual proliferation was mostly abrogated by anti-IL-4 mAb treatment (Fig. 5A). Tr1 cells have been defined to exert the suppressor activity via IL-10 *in vitro* and *in vivo* [3]. In contrast, the suppressor activity of $CD4^+CD25^-PD\text{-}1^+$ cells was not abrogated by addition of anti-IL-10 mAb (Fig. 5A), but was partially abolished by addition of anti-CTLA-4 mAb (Fig. 5B). These results suggest that the *in*

vitro suppressor activity of the $CD4^+CD25^-PD\text{-}1^+$ cells might be exerted in a manner dependent on $FoxP3^+$ T_R cells, but independently of the contaminating Th2 and Tr1 cells. In addition, it is possible that TGF-β produced by $CD4^+CD25^-PD\text{-}1^+$ cells (Fig. 2D) might also contribute to the suppression by these cells. Furthermore, it should be emphasized that our $CD4^+CD25^-PD\text{-}1^+$ cells are a heterogeneous population, which uniquely consisted of $FoxP3^+$ T_R cells, IL-4-producing Th2 cells, and IL-10-producing Tr1 cells.

It has been well characterized that the $CD4^+CD45RB^{low}$ population exhibits T_R activity *in vitro* and prevents the development of $CD4^+CD45RB^{high}$ T cell-induced colitis in SCID mice [2]. It has also been reported that $CD4^+CD25^+$ cells constitute the major T_R population among $CD4^+CD45RB^{low}$ cells [6]. Our present study showed that the $CD25^-PD\text{-}1^+$ cells constituted a substantial population (4.6±0.9%) of $CD4^+CD45RB^{low}$ cells, which expressed FoxP3 and exerted a significant T_R activity *in vitro* and *in vivo*. These results suggest that the $CD25^-PD\text{-}1^+$ population may also partly contribute to the suppressor activity of $CD4^+CD45RB^{low}$ cells *in vitro* and *in vivo*.

We recently identified a subpopulation of $CD4^+CD25^-$ cells expressing GITR, which exhibited T_R activity *in vitro* and prevented the development of $CD4^+CD45RB^{high}$ T cell-induced colitis in SCID mice [18]. Our present study showed that only 18% of $GITR^+$ cells expressed PD-1, and 25% of $PD\text{-}1^+$ cells expressed GITR among $CD4^+CD25^-$ cells (Fig. 4A). Moreover, the $CD4^+CD25^-PD\text{-}1^+$ cells exhibited the T_R activity *in vitro*, irrespective of GITR expression (Fig. 4C). These results suggest that the $CD4^+CD25^-GITR^+$ T_R population and the $CD4^+CD25^-PD\text{-}1^+$ T_R population only partially overlap and that each population can exert the T_R activity independently.

The *in vivo* studies (Figs. 6, 7) demonstrated that $CD4^+CD45RB^{low}CD25^-PD\text{-}1^+$ cells, as well as $CD4^+CD45RB^{low}CD25^+$ cells, could suppress the development of chronic colitis induced by adoptive transfer of $CD4^+CD45RB^{high}$ T cells into SCID mice. In this colitis model, the $CD4^+CD45RB^{high}$ T cells contain pathogenic T cells that differentiate into Th1 cells upon exposure to bacterial flora [1]. It has been well characterized that co-transfer of $CD4^+CD45RB^{low}$ T cells suppresses the development of colitis [2]. Although recent studies have shown that the $CD4^+CD25^+$ T_R cells are the major component of $CD4^+CD45RB^{low}$ suppressor cells [6], our present results show that $CD4^+CD25^-PD\text{-}1^+$ cells constitute a substantial population among $CD4^+CD45RB^{low}$ cells (Figs. 3A, 7). The $CD4^+CD45RB^{low}CD25^-PD\text{-}1^+$ cells as well as $CD4^+CD45RB^{low}CD25^+$ cells, but not $CD4^+CD45RB^{low}CD25^-PD\text{-}1^-$ cells, inhibited the expansion/infiltration of $CD4^+CD45RB^{high}$ T cells (Fig. 7E) and their differentiation into Th1 cells (Fig. 6G). These results suggest that the $CD4^+CD45RB^{low}CD25^-PD\text{-}1^+$ cells are also a substantial component of the $CD4^+CD45RB^{low}$ T_R cells.

Interestingly, the suppressive effect of $CD4^+CD25^-PD\text{-}1^+$ cells on $CD4^+CD45RB^{high}$ T cell-induced colitis was totally abrogated by administration of a blocking anti-CTLA-4 mAb (Fig. 8). It has been demonstrated that CTLA-4 also plays a critical role in the suppression of colitis by the $CD4^+CD25^+$ T_R cells [6]. However, how CTLA-4 mediates this suppression remains controversial. A previous paper suggested that CTLA-4-mediated signaling may induce IL-10 or TGF-β production by the $CD4^+CD25^+$ T_R cells [22]. Alternatively, CTLA-4 in the T_R cells may compete with CD28 on responder T cells for B7 on APC. Moreover, a recent study has suggested that engagement of B7 on APC by CTLA-4 in the $CD4^+CD25^+$ T_R cells induces the production of tryptophan-catabolizing enzymes by APC, which suppresses responder T cell expansion by tryptophan depletion and apoptosis [23]. A similar mechanism may be used by the $CD4^+CD25^-PD\text{-}1^+$ T_R cells. In contrast, a blocking anti-PD-1 mAb (RMP1–14) did not affect the suppressor activity of $CD4^+CD25^-PD\text{-}1^+$ cells *in vitro* or *in vivo* (Figs. 5, 8). This is not likely to be due to an inability of RMP1–14 to block PD-1, since this mAb blocked the PD-L1-dependent induction of T_R cells by intratracheal delivery of alloantigen [24]. We have also recently observed that RMP1–14, but not RMP1–30, exacerbates experimental autoimmune encephalomyelitis (EAE) and graft-versus-host disease (GVHD) (H.Y., unpublished data), as we previously reported with a hamster anti-mouse PD-1 mAb (J43) [25, 26]. Therefore, PD-1 expressed on $CD4^+CD25^-PD\text{-}1^+$ cells may not be functionally involved in their suppressor activity. This notion is also consistent with the equivalent suppressor activity of $CD4^+CD25^+PD\text{-}1^-$ and $CD4^+CD25^+PD\text{-}1^+$ cells *in vitro* (Fig. 2C) and *in vivo* (Fig. 6). However, it remains still possible that PD-1 may be functionally involved in the development of $CD4^+CD25^-PD\text{-}1^+$ and $CD4^+CD25^+PD\text{-}1^+$ T_R cells, since we recently demonstrated that induction of T_R cells by intratracheal delivery of alloantigen was dependent on the PD-1/PD-L1 interaction [24]. In this context, it is noteworthy that PD-1-deficient mice spontaneously develop autoimmune diseases [11, 12]. Therefore, PD-1 may be functionally involved in the development of $PD\text{-}1^+$ T_R cells that control autoimmune responses.

In conclusion, the present study has demonstrated that the $CD4^+CD25^-PD\text{-}1^+$ cells in the spleen of naive mice represent a substantial population of T_R cells that exerts a CTLA-4-dependent suppressor activity in a chronic colitis model. They may also exert regulatory activities via IL-4, IL-10, and TGF-β production in other systems. Further studies are now under way to clarify

their developmental process and pathophysiological role in regulating immune responses to endogenous or exogenous antigens.

Materials and methods

Mice

Female BALB/c and C.B17-scid/scid (SCID) mice were purchased from Japan Clea (Tokyo, Japan). Donors and recipients were sex matched and were used at 6–12 weeks of age according to the guidelines of the Institutional Committee on Animal Research in the Tokyo Medical and Dental University.

Antibodies

The following mAb were used: FcγR (CD16/32)-blocking mAb (2.4G2), FITC- and CyChrome-conjugated anti-mouse CD4 (RM4–5), FITC-conjugated anti-mouse CD25 (7D4), PE-conjugated anti-CTLA-4 (UC10-4F10-11), PE-conjugated anti-mouse CD103 (DATK32), PE-conjugated anti-mouse CD45RB (16A), PE-conjugated anti-mouse CD44 (IM7), PE-conjugated anti-mouse CD62L (MEL-14), PE-conjugated anti-mouse CD69 (H1.2F3), PE-conjugated streptavidin, and CyChrome-conjugated streptavidin were purchased from BD PharMingen (San Diego, CA). PE-conjugated anti-GITR antibody (108619) was purchased from R&D Systems (Minneapolis, MN). Two rat IgG2a anti-mouse PD-1 mAb (RMP1–14 and RMP1–30) were newly generated against mouse PD-1 transfectants (A.K. and H.Y.; details will be described elsewhere). RMP1–14, but not RMP1–30, blocks the interaction of PD-1 with its ligands (PD-L1 and PD-L2). These mAb were purified from ascites and biotinylated by standard methods. Blocking mAb against CTLA-4 (UC10–4F10) was prepared from a hybridoma generously provided by J. A. Bluestone (UCSF). Blocking mAb against IL-4 (11B11) and IL-10 (JES5–2A5) were prepared from the corresponding hybridomas from ATCC.

Flow cytometric analysis

To examine the expression of cell surface molecules, cells were first pre-incubated with FcγR-blocking mAb and then stained with CyChrome-conjugated anti-CD4 mAb, FITC-conjugated anti-CD25 mAb, and PE-conjugated anti-α_E, anti-CD45RB, anti-CD62L, anti-CD44, or anti-CD69 mAb or biotinylated anti-PD-1 mAb, followed by PE-conjugated streptavidin. For intracellular staining with PE-conjugated anti-CTLA-4 mAb, the cells were fixed and permeabilized with Cytofix/Cytoperm (BD PharMingen). Staining and washing were performed in Perm/Wash Buffer (BD PharMingen). For intracellular staining for IL-4 and IL-10, cells were stimulated with plate-bound anti-CD3 mAb (5 μg/ml) + soluble anti-CD28 mAb (2 μg/ml) for 48 h, and 5 μg/ml brefeldin A (GolgiPlug; BD PharMingen) was added for the last 4 h. The stimulated cells were fixed, permeabilized, and stained with PE-conjugated anti-IL-4 mAb (11B11; BD PharMingen) and FITC-conjugated anti-IL-10 mAb (JE55–16E3; BD PharMingen) as described above.

Purification of T cell subsets

$CD4^+$ T cells were isolated from BALB/c splenocytes using the anti-CD4 (L3T4) MACS system (Miltenyi Biotec, Auburn, CA) according to the manufacturer's instructions. The enriched $CD4^+$ T cells (97–98% pure as estimated by flow cytometry) were then stained with PE-conjugated anti-mouse CD4 mAb and FITC-conjugated anti-CD45RB mAb for the isolation of $CD4^+CD45RB^{high}$ and $CD4^+CD45RB^{low}$ T cells; FITC-conjugated anti-CD25 mAb and biotinylated anti-PD-1 mAb (RMP1–30) followed by PE-conjugated streptavidin for the isolation of $CD4^+CD25^-PD\text{-}1^-$, $CD4^+CD25^+PD\text{-}1^-$, $CD4^+CD25^-PD\text{-}1^+$ and $CD4^+CD25^+PD\text{-}1^+$ T cells; CyChrome-conjugated anti-CD25 mAb, FITC-conjugated anti-CD45RB mAb and biotinylated anti-PD-1 mAb followed by PE-conjugated streptavidin for the isolation of $CD4^+CD45RB^{low}CD25^-PD\text{-}1^+$ and $CD4^+CD45RB^{low}CD25^-PD\text{-}1^-$ T cells; or CyChrome-conjugated anti-CD25 mAb, PE-conjugated anti-GITR mAb and biotinylated anti-PD-1 mAb followed by CyChrome-conjugated streptavidin for the isolation of $CD4^+CD25^-PD\text{-}1^+GITR^+$ and $CD4^+CD25^-PD\text{-}1^+GITR^-$ T cells. These subpopulations were isolated by sorting on a FACS Vantage (Becton Dickinson). All populations were >98.0% pure upon reanalysis.

In vitro T_R functional analysis

As APC, $CD4^-$ cells were prepared from BALB/c splenocytes by depleting $CD4^+$ cells with anti-CD4 MACS, and treated with 50 μg/ml mitomycin C (MMC) for 45 min at 37°C. $CD4^+CD25^-PD\text{-}1^-$, $CD4^+CD25^-PD\text{-}1^+$, $CD4^+CD25^+PD\text{-}1^-$, and $CD4^+CD25^+PD\text{-}1^+$ cells (1×10^4) were cultured with MMC-treated $CD4^-$ cells (5×10^4) in round-bottom 96-well plates in RPMI 1640 medium containing 10% FCS, 100 IU/ml penicillin, 100 μg/ml streptomycin, 2 mM glutamine, 1 mM sodium pyruvate, 50 μM 2-mercaptoethanol (complete medium), and supplemented with 1 μg/ml anti-CD3 mAb (145–2C11; BD PharMingen). In co-culture experiments, $CD4^+CD25^-PD\text{-}1^-$, $CD4^+CD25^-PD\text{-}1^+$, $CD4^+CD25^+PD\text{-}1^-$, and $CD4^+CD25^+PD\text{-}1^+$ T cells (1×10^4, as T_R cells) were cultured with $CD4^+CD25^-PD\text{-}1^-$ T cells (1×10^4, as responders) and MMC-treated $CD4^-$ cells (5×10^5, as APC) in the presence of anti-CD3 mAb (1 μg/ml). In some experiments, $CD4^+CD45RB^{low}CD25^-PD\text{-}1^+$ and $CD4^+CD45RB^{low}CD25^-PD\text{-}1^-$ T cells, or $CD4^+CD25^-PD\text{-}1^+GITR^+$ and $CD4^+CD25^-PD\text{-}1^+GITR^-$ T cells were used as T_R. To determine proliferation rates, each well was pulsed with 1 μCi of [^{3}H]thymidine (NEN, Boston, MA) for the last 9 h of a 72-h culture. In some experiments, blocking mAb against IL-4, IL-10, CTLA-4, and PD-1 were added at 50 μg/ml from the beginning of culture. To determine cytokine production, freshly isolated $CD4^+CD25^-PD\text{-}1^-$, $CD4^+CD25^-PD\text{-}1^+$, $CD4^+CD25^+PD\text{-}1^-$, and $CD4^+CD25^+PD\text{-}1^+$ T cells (1×10^5 cells/well) were cultured in complete medium or a serum-free medium (Nutridoma SP; Roche Molecular Biochemicals, Indianapolis, IN) for TGF-β in flat-bottom 96-well plates, and stimulated with 5 μg/ml plate-bound anti-CD3 mAb + 2 μg/ml soluble anti-CD28 mAb (37.51; BD PharMingen). Supernatants were collected after 24 h for IL-2, 48 h for IL-4, IL-10, and IFN-γ, and 72 h for TGF-β. Total TGF-β in the acidified supernatants was determined by using TGF-β1 Emax Immunoassay Kit (Prome-

ga, Madison, WI). Other cytokines were measured by using specific ELISA kits (R&D Systems).

RT-PCR

Total cellular RNA was extracted from 5×10^5 cells using the RNeasy Mini Kit (Qiagen, Valencia, CA). RNA (150 ng) was reverse transcribed using the Superscript First-Strand Synthesis System (Invitrogen). FoxP3 levels were measured by dual-labeled probe RT-PCR using a Smart Cycler (Cepheid, Sunnyvale, CA). The PCR contained 0.3 mM each of the primers, 0.2 mM probe, 3 mM $MgCl_2$ and 0.75 U Platinum Taq polymerase (Invitrogen). The primer sequences were designed to contain two exons to avoid amplification of genomic DNA: FoxP3, 5′-CAG CTG CCT ACA GTG CCC CTA G-3′ and 5′-CAT TTG CCA GCA GTG GGT AG-3′ [8]; glyceraldehyde-3-phosphate dehydrogenase (G3PDH), 5′-TGA AGG TCG GTG TGA ACG GAT TTG GC-3′ and 5′-CAT GTA GGC CAT GAG GTC CAC CAC-3′. PCR cycling conditions consisted of 95°C for 6 min, followed by 40 cycles of 95°C for 15 s, 60°C for 30 s and 72°C for 30 s. Critical threshold (CT) values were compared against a standard curve to estimate starting amounts of mRNA, and the relative expression of FoxP3 mRNA among samples was estimated by normalizing these values against 18S rRNA CT values generated using a pre-optimized 18S rRNA primers and probe set (Applied Biosystems, Foster City, CA). The FoxP3/G3PDH gene expression ratio of $CD4^+CD25^-PD\text{-}1^-$ cells was given an arbitrary value of 1.0 to determine relative expression levels.

In vivo experiments

Chronic colitis was induced by i.p. injection of $CD4^+$ $CD45RB^{high}$ splenic T cells (3×10^5) from BALB/c mice into C.B17-SCID mice as described [27]. To examine the regulatory function, $CD4^+CD25^-PD\text{-}1^-$, $CD4^+CD25^-PD\text{-}1^+$, $CD4^+CD25^+$ $PD\text{-}1^-$, or $CD4^+CD25^+PD\text{-}1^+$ splenic T cells (1×10^5) were co-injected with $CD4^+CD45RB^{high}$ cells (3×10^5 cells). Some groups were i.p. administrated with 200 μg blocking anti-CTLA-4 mAb (UC10–4F10), blocking anti-PD-1 mAb (RMP1–14), non-blocking anti-PD-1 mAb (RMP1–30), or control IgG, three times per week for 6 weeks from the day of T cell transfer. The recipient SCID mice after T cell transfer were weighed initially and then three times per week. They were also observed for clinical signs such as hunched posture, piloerection, diarrhea, and blood in the stool. In another set of experiments, to assess whether suppression of colitis is restricted to a subpopulation of $CD4^+CD45RB^{low}PD\text{-}1^+$ $CD25^-$ cells but not $CD4^+CD45RB^{low}PD\text{-}1^-CD25^-$ cells, $CD4^+CD45RB^{low}CD25^-PD\text{-}1^-$, $CD4^+CD45RB^{low}CD25^-PD\text{-}1^+$, or $CD4^+CD25^+$ splenic T cells (1×10^5 each) were co-injected with $CD4^+CD45RB^{high}$ cells (3×10^5 cells). The mice were sacrificed 7 weeks after T cell transfer and assessed for a clinical score that is the sum of four parameters as follows: hunching and wasting, 0 or 1; colon thickening, 0–3 (0, no colon thickening; 1, mild thickening; 2, moderate thickening; 3, extensive thickening); and stool consistency, 0–3 (0, normal beaded stool; 1, soft stool; 2, diarrhea; 3, bloody stool). Tissue samples were fixed in 6% neutral-buffered formalin. Paraffin-embedded sections (5 μm) were stained with hematoxylin and eosin. Three tissue samples from the proximal, middle, and distal parts of the colon were prepared. Histological scores were evaluated in a blind manner as described [27].

Characterization of LP mononuclear cells

LP mononuclear cells were prepared essentially as described [27]. To measure cytokine production, LP $CD4^+$ T cells (1×10^5) were cultured in flat-bottom 96-well plates with 5 μg/ml plate-bound anti-CD3 mAb and 2 μg/ml soluble anti-mouse CD28 mAb for 48 h. Cytokines in the supernatants were measured by ELISA.

Statistical analysis

The results were expressed as the mean ± standard deviation (SD). Groups of data were compared by Mann-Whitney U test. Differences were considered to be statistically significant when $p<0.05$.

Acknowledgements: This work was supported in part by grants-in-aid from the Japanese Ministry of Education, Culture and Science and the Japanese Ministry of Health and Welfare.

References

1 **Singh, B., Read, S., Asseman, C., Malmstrom, V., Mottet, C., Stephens, L. A., Stepankova, R., Tlaskalova, H. and Powrie, F.,** Control of intestinal inflammation by regulatory T cells. *Immunol. Rev.* 2001. **182:** 190–200.

2 **Powrie, F., Leach, M. W., Mauze, S., Caddle, L. B. and Coffman, R. L.,** Phenotypically distinct subsets of $CD4^+$ T cells induce or protect from chronic intestinal inflammation in C.B-17 scid mice. *Int. Immunol.* 1993. **5:** 1461–1471.

3 **Groux, H., O'Garra, A., Bigler, M., Rouleau, M., Antonenko, S., de Vries, J. E. and Roncarolo, M. G.,** A $CD4^+$ T cell subset inhibits antigen-specific T cell responses and prevents colitis. *Nature* 1997. **389:** 737–742.

4 **Chen, Y., Kunchroo, V. K., Inobe, J., Hafler, D. A. and Weiner, H. L.,** Regulatory T cell clones induced by oral tolerance: suppression of autoimmune encephalomyelitis. *Science* 1994. **265:** 1237–1240.

5 **Sakaguchi, S., Sakaguchi, N., Asano, M., Itoh, M. and Toda, M.,** Immunological self-tolerance maintained by activated T cells expressing IL-2 receptor alpha chains (CD25). Breakdown of a single mechanism of self-tolerance causes various autoimmune diseases. *J. Immunol.* 1995. **155:** 1151–1564.

6 **Read, S., Malmstrom, V. and Powrie, F.,** Cytotoxic T lymphocyte-associated antigen 4 plays an essential role in the function of $CD25^+CD4^+$ regulatory cells that control intestinal inflammation. *J. Exp. Med.* 2000. **193:** 295–302.

7 **Takahashi, T., Tagami, T., Yamazaki, S., Ueda, T., Shimizu, J., Sakaguchi, N., Mak, T. W. and Sakaguchi, S.,** Immunologic self-tolerance maintained by $CD4^+CD25^+$ regulatory T cells constitutively expressing cytotoxic T lymphocyte-associated antigen 4. *J. Exp. Med.* 2000. **192:** 303–310.

8 **Hori, S., Nomura, T. and Sakaguchi, S.,** Control of regulatory T cell development by the transcription factor Foxp3. *Science* 2003. **299:** 1057–1061.

9 **Ishida, Y., Agata, Y., Shibahara, K. and Honjo, T.,** Induced expression of PD-1, a novel member of the immunoglobulin gene superfamily, upon programmed cell death. *EMBO J.* 1992. **11:** 3887–3895.

10 **Freeman, G. J., Long, A. J., Iwai, Y., Bourque, K., Chernova, T., Nishimura, H., Fitz, L. J., Malenkovich, N., Okazaki, T., Byrne, M. C., Horton, H. F., Fouser, L., Carter, L., Ling, V., Bowman, M. R., Carreno, B. M., Collins, M., Wood, C. R. and Honjo, T.,** Engagement of the PD-1

immunoinhibitory receptor by a novel B7 family member leads to negative regulation of lymphocyte activation. *J. Exp. Med.* 2000. **192:** 1027–1034.

11 **Nishimura, H., Okazaki, T., Tanaka, Y., Nakatani, K., Hara, M., Matsumori, A., Sasayama, S., Mizoguchi, A., Hiai, H., Minato, N. and Honjo, T.,** Autoimmune dilated cardiomyopahty in PD-1 receptor-deficient mice. *Science* 2001. **291:** 319–322.

12 **Nishimura, H., Nose, M., Hiai, H., Minato, N. and Honjo, T.,** Development of lupus-like autoimmune diseases by disruption of the PD-1 gene encoding an ITIM motif-carrying immunoreceptor. *Immunity* 1999. **11:** 141–151.

13 **Nishimura, H. and Honjo, T.,** PD-1: an inhibitory immunoreceptor involved in peripheral tolerance. *Trends Immunol.* 2001. **22:** 265–268.

14 **Stephens, L. A. and Mason, D.,** CD25 is a marker for $CD4^+$ thymocytes that prevent autoimmune diseases in rats, but peripheral T cells with this function are found in both $CD25^+$ and $CD25^-$ subpopulations. *J. Immunol.* 2000. **165:** 3105–3110.

15 **Annacker, O., Pimenta-Araujo, R., Burlen-Defranoux, O., Barbosa, T. C., Cumano, A. and Bandeira, A.,** $CD25^+CD4^+$ T cells regulate the expansion of peripheral CD4 T cells through the production of IL-10. *J. Immunol.* 2001. **166:** 3008–3018.

16 **Lehmann, J., Huehn, J., de la Rosa, M., Maszyna, F., Kretschmer, U., Krenn, V., Brunner, M. and Hamann, A.,** Expression of the integrin $\alpha_E\beta_7$ identifies unique subsets of $CD25^+$ as well as $CD25^-$ regulatory T cells. *Proc. Natl. Acad. Sci. USA* 2002. **99:** 13031–13036.

17 **Oida, T., Zhang, X., Goto, M., Hachimura, S., Totsuka, M., Kaminogawa, S., and Weiner, H. L.,** $CD4^+CD25^-$ T cells that express latency-associated peptide on the surface suppress $CD4^+CD45RB^{high}$-induced colitis by a TGF-beta-dependent mechanism. *J. Immunol.* 2003. **170:** 2516–2522.

18 **Uraushihara, K., Kanai, T., Ko, K., Totsuka, T., Makita, S., Iiyama, R., Nakamura, T. and Watanabe, M.,** Regulation of murine inflammatory bowel disease by $CD25^+$ and $CD25^-$ $CD4^+$ glucocorticoid-induced TNF receptor family-related $gene^+$ regulatory T cells. *J. Immunol.* 2003. **171:** 708–716.

19 **Shimizu, J., Yamazaki, S., Takahashi, T., Ishida, Y. and Sakaguchi, S.,** Stimulation of $CD25^+CD4^+$ regulatory T cells through GITR breaks immunological self-tolerance. *Nat. Immunol.* 2002. **3:** 135–142.

20 **Walker, M. R., Kasprowicz, D. J., Gersuk, V. H., Benard, A., Van Landeghen, M., Buckner, J. H. and Ziegler, S. F.,** Induction of FoxP3 and acquisition of T regulatory activity by stimulated human $CD4^+CD25^-$ T cells. *J. Clin. Invest.* 2003. **112:** 1437–1443.

21 **Chen, W., Jin, W., Hardegen, N., Lei, K. J., Li, L., Marinos, N., McGrady, G. and Wahl, S. M.,** Conversion of peripheral $CD4^+CD25^-$ naive T cells by $CD4^+CD25^+$ regulatory T cells by TGF-β induction of transcription factor FoxP3. *J. Exp. Med.* 2003. **198:** 1875–1886.

22 **Nakamura, K., Kitani, A. and Strober, W.,** Cell contact-dependent immunosuppression by $CD4^+CD25^+$ regulatory T cells is mediated by cell surface-bound transforming growth factor β. *J. Exp. Med.* 2001. **194:** 629–644.

23 **Fallarino, F., Grohmann, U., Hwang, K. W., Orabona, C., Vacca, C., Bianchi, R., Belladonna, M. L., Fioretti, M. C., Alegre, M. L. and Puccetti, P.,** Modulation of tryptophan catabolism by regulatory T cells. *Nat. Immunol.* 2003. **4:** 1206–1212.

24 **Aramaki, O., Shirasugi, N., Takayama, T., Shimazu, M., Kitajima, M., Ikeda, Y., Azuma, M., Okumura, K., Yagita, H. and Niimi, M.,** Programmed death-1-programmed death-L1 interaction is essential for induction of regulatory cells by intratracheal delivery of alloantigen. *Transplantation* 2004. **77:** 6–12.

25 **Salama, A. D., Chitnis, T., Imitola, J., Ansari, M. J., Akiba, H., Tushima, F., Azuma, M., Yagita, H., Sayegh, M. H. and Khoury, S. J.,** Critical role of the programmed death-1 (PD-1) pathway in regulation of experimental autoimmune encephalomyelitis. *J. Exp. Med.* 2003. **198:** 71–78.

26 **Blazar, B. R., Carreno, B. M., Panoskaltsis-Mortani, A., Carter, L., Iwai, Y., Yagita, H., Nishimura, H. and Taylor, P. A.,** Blockade of programmed death-1 engagement accelerates graft-versus-host disease lethality by an IFN-γ-dependent mechanism. *J. Immunol.* 2003. **171:** 1272–1277.

27 **Kanai, T., Totsuka, T., Uraushihara, K., Makita, S., Nakamura, T., Koganei, K., Fukushima, T., Akiba, H., Yagita, H., Okumura, K. et al.,** Blockade of B7-H1 suppresses the development of chronic intestinal inflammation. *J. Immunol.* 2003. **171:** 4156–4163.

Abnormally Differentiated Subsets of Intestinal Macrophage Play a Key Role in Th1-Dominant Chronic Colitis through Excess Production of IL-12 and IL-23 in Response to Bacteria[1]

Nobuhiko Kamada,* Tadakazu Hisamatsu,* Susumu Okamoto,* Toshiro Sato,* Katsuyoshi Matsuoka,* Kumiko Arai,* Takaaki Nakai,* Akira Hasegawa,* Nagamu Inoue,* Noriaki Watanabe,† Kiyoko S. Akagawa,‡ and Toshifumi Hibi[2]*

Disorders in enteric bacteria recognition by intestinal macrophages (Mϕ) are strongly correlated with the pathogenesis of chronic colitis; however the precise mechanisms remain unclear. The aim of the current study was to elucidate the roles of Mϕ in intestinal inflammation by using an IL-10-deficient (IL-10$^{-/-}$) mouse colitis model. GM-CSF-induced bone marrow-derived Mϕ (GM-Mϕ) and M-CSF-induced bone marrow-derived Mϕ (M-Mϕ) were generated from bone marrow CD11b$^+$ cells. M-Mϕ from IL-10$^{-/-}$ mice produced abnormally large amounts of IL-12 and IL-23 upon stimulation with heat-killed whole bacteria Ags, whereas M-Mϕ from wild-type (WT) mice produced large amounts of IL-10 but not IL-12 or IL-23. In contrast, IL-12 production by GM-Mϕ was not significantly different between WT and IL-10$^{-/-}$ mice. In ex vivo experiments, cytokine production ability of colonic lamina propria Mϕ (CLPMϕ) but not splenic Mϕ from WT mice was similar to that of M-Mϕ, and CLPMϕ but not splenic Mϕ from IL-10$^{-/-}$ mice also showed abnormal IL-12p70 hyperproduction upon stimulation with bacteria. Surprisingly, the abnormal IL-12p70 hyperproduction from M-Mϕ from IL-10$^{-/-}$ mice was improved by IL-10 supplementation during the differentiation process. These results suggest that CLPMϕ and M-Mϕ act as anti-inflammatory Mϕ and suppress excess inflammation induced by bacteria in WT mice. In IL-10$^{-/-}$ mice, however, such Mϕ subsets differentiated into an abnormal phenotype under an IL-10-deficient environment, and bacteria recognition by abnormally differentiated subsets of intestinal Mϕ may lead to Th1-dominant colitis via IL-12 and IL-23 hyperproduction. Our data provide new insights into the intestinal Mϕ to gut flora relationship in the development of colitis in IL-10$^{-/-}$ mice. *The Journal of Immunology,* **2005, 175: 6900–6908.**

Macrophages (Mϕ),[3] the major population of tissue-resident mononuclear phagocytes, play key roles in bacterial recognition and elimination as well as in polarization of innate and adaptive immunities. Mϕ are activated by microbial pathogen-associated molecular patterns (PAMPs) through pattern-recognition receptors, such as TLRs (1, 2), and produce proinflammatory cytokines such as IL-12 and IL-23, thereby leading to development of Th1 immunity (3). Besides these classical antibacterial immune roles, it has recently become evident that Mϕ also play important roles in homeostasis maintenance, such as inflammation dampening, via production of anti-inflammatory cytokines such as IL-10 and TGF-β, debris scavenging, angiogenesis, and wound repair (4–6). IL-10 and IL-12 are two key players in these processes, usually acting in opposition, with IL-10 inhibiting IL-12 production. Therefore, loss of balance between IL-12 and IL-10 can lead to disproportionate pathology or immunosuppression.

Although precise etiologies of inflammatory bowel diseases (IBDs) including Crohn's disease and ulcerative colitis remain unclear, pathogenic roles of the gut flora in initiation and perpetuation of intestinal inflammation have been proposed (7). Recently, it has become evident that abnormal innate immune responses to bacteria are responsible for the pathogenesis of IBD. For instance, mutations in nucleotide-binding oligomerization domain (NOD)2 highly correlated with disease incidence in a substantial subgroup of patients with Crohn's disease (8, 9). NOD2 mutant Mϕ were reported to produce large amounts of IL-12 in response to stimulation with microbial components, compared with wild-type (WT) cells, and to promote Th1 immunity (10). Thus, disorders in bacterial recognition by Mϕ strongly correlate with pathogenesis of IBDs (11–13).

IL-10-deficient (IL-10$^{-/-}$) mice develop spontaneous chronic colitis and are widely used as a colitis animal model for human IBDs (14). IL-10$^{-/-}$ mice show Th1 polarized immunity upon exposure to bacteria, whereas germfree conditions prevent development of intestinal inflammation (15), and treatment with antibiotics attenuates intestinal inflammation (16, 17). These facts suggest that enteric bacteria play essential roles in onset and development of colitis in IL-10$^{-/-}$ mice, similar to human IBDs. Recently, the following pathogenic aspects of Mϕ in IL-10$^{-/-}$ mice have been reported: APC such as Mϕ and dendritic cells (DC), from IL-10$^{-/-}$ mice were potent activators of Th1 responses

*Department of Internal Medicine, School of Medicine, Keio University, †Department of Internal Medicine, Kitasato Institute Hospital, and ‡Department of Immunology, National Institute of Infectious Diseases, Tokyo, Japan

Received for publication June 14, 2005. Accepted for publication September 14, 2005.

The costs of publication of this article were defrayed in part by the payment of page charges. This article must therefore be hereby marked *advertisement* in accordance with 18 U.S.C. Section 1734 solely to indicate this fact.

[1] This work was supported in part by grants-in-aid from the Japanese Ministry of Education, Culture, and Science, the Japanese Ministry of Labor, Health, and Welfare, Keio University, and Keio University Medical Fund.

[2] Address correspondence and reprint requests to Dr. Toshifumi Hibi, Department of Internal Medicine, School of Medicine, Keio University, 35 Shinano machi, Shinjuku-ku, Tokyo 160-8582, Japan. E-mail address: thibi@sc.itc.keio.ac.jp

[3] Abbreviations used in this paper: Mϕ, macrophage; WT, wild type; DC, dendritic cell; IBD, inflammatory bowel disease; NOD, nucleotide-binding oligomerization domain; BM, bone marrow; M-Mϕ, M-CSF-induced BM-derived Mϕ; GM-Mϕ, GM-CSF-induced BM-derived Mϕ; PGN, peptidoglycan; MDP, muramyl-dipeptide; PAMP, pathogen-associated molecular pattern; MOI, multiplicity of infection; CBA, cytometric beads array; CLPMϕ, colonic lamina propria macrophage.

0022-1767/05/$02.00

from naive or immune T cells (18, 19); Mϕ from IL-$10^{-/-}$ mice were hyperreactive to microbial components (20); and Mϕ depletion prevented chronic colitis in IL-$10^{-/-}$ mice (21). Based on these reports, Mϕ and DC are considered to play key roles in the pathogenesis of colitis in IL-$10^{-/-}$ mice, although mechanisms for bacterial recognition by APC that induces a Th1 bias and development of intestinal inflammation remain unclear. Previous studies suggested that IL-12 was crucial for development of colitis in IL-$10^{-/-}$ mice because mice deficient for both IL-10 and IL-12p40 showed no intestinal inflammation, and treatment with anti-IL-12p40 Abs markedly reduced intestinal inflammation (22, 23). Until now, however, how IL-10 deficiency affects IL-12 production from Mϕ in mice has not been thoroughly analyzed.

In the present study, we examined whether IL-10-deficient conditions affected differentiation and functions of bone marrow (BM)-derived Mϕ subsets and intestinal Mϕ, and investigated how bacteria recognition by Mϕ induced a Th1 polarization and intestinal inflammation in IL-$10^{-/-}$ mice. We found that M-CSF-induced BM-derived Mϕ (M-Mϕ) and intestinal Mϕ, but not GM-CSF-induced BM-derived Mϕ (GM-Mϕ) or splenic Mϕ from IL-$10^{-/-}$ mice showed abnormal hyperproduction of IL-12 and IL-23 upon stimulation with bacteria. More importantly, our results suggested that endogenous IL-10 played an essential role in differentiation of the anti-inflammatory Mϕ subset induced by M-CSF.

Materials and Methods

Reagents

Recombinant mouse GM-CSF, M-CSF, and IL-10 were purchased from R&D Systems. Gel filtration grade LPS (*Escherichia coli* O111:B4), muramyl-dipeptide (MDP), and *Staphylococcus aureus* peptidoglycan (PGN) were obtained from Sigma-Aldrich. Pam_3CSK_4 and *E. coli* ssDNA were obtained from InvivoGen.

Bacteria heat-killed Ags

A Gram-negative nonpathogenic strain of *E. coli* (25922; American Type Culture Collection (ATCC)) was cultured in Luria-Bertani medium, and a Gram-positive strain of *Enterococcus faecalis* (29212; ATCC) was cultured in brain-heart infusion medium. Bacteria were harvested and washed twice with ice-cold PBS. Then, bacterial suspensions were heated at 80°C for 30 min, washed, resuspended in PBS, and stored at −80°C. Complete killing was confirmed by 72 h incubation at 37°C on plate medium.

Mice

Specific pathogen-free WT C57BL/6J mice were purchased from Charles River Breeding Laboratories. WT and IL-$10^{-/-}$ (C57BL/6J background) mice were housed under specific pathogen-free conditions at the animal center of Kitasato Institute Hospital and Keio University (Tokyo, Japan). All experiments using mice were approved by and performed according to the guidelines of the animal committee of Keio University and Kitasato Institute Hospital.

Preparation of BM-derived Mϕ

BM cells were isolated from femora of 7- to 12-wk-old mice. After separation of BM mononuclear cells by gradient centrifugation, $CD11b^+$ cells were purified using a magnetic cell separation system (MACS; Miltenyi Biotec) with anti-mouse CD11b microbeads. To generate BM-derived GM-Mϕ and M-Mϕ, $CD11b^+$ cells (5×10^5 cells/ml) were cultured for 7 days with GM-CSF (20 ng/ml) and M-CSF (20 ng/ml), respectively. In some experiments, to determine effects of IL-10 during differentiation of M-Mϕ, BM $CD11b^+$ cells from IL-$10^{-/-}$ mice were cultured with M-CSF and various concentrations of exogenous IL-10. After differentiation, cells were washed three times with HBSS to remove residual IL-10.

Flow cytometry analysis

Day 7 BM-derived GM-Mϕ and M-Mϕ were harvested with EDTA and washed with ice-cold PBS. Then, cells were preincubated with 1 μg/ml mAb CD16/CD32 to block FcγR, and stained with mAbs CD11b, Gr-1, TLR4/MD2, or TLR2 (all from eBiosciences), mAbs CD80 or CD86 (both from BD Pharmingen) or their isotype control Abs for 20 min at 4°C. After staining, cells were washed with PBS, stained with propidium iodide, and analyzed using a FACSCalibur (BD Pharmingen). The CellQuest software was used for data analysis.

Activation of BM-derived Mϕ by PAMPs

Day 7 BM-derived GM-Mϕ and M-Mϕ were harvested, plated on 96-well tissue culture plates (1×10^5 cells/well) in RPMI 1640 medium supplemented with 10% FBS, antibiotics, and 20 ng/ml GM-CSF or M-CSF, and incubated for 12–16 h. Before each experiment, Mϕ were washed three times with HBSS (Sigma-Aldrich) to completely remove secreted or supplemented cytokines from the supernatant, and were stimulated with either LPS (100 ng/ml), PGN (2 μg/ml), Pam_3CSK_4 (500 ng/ml), *E. coli* ssDNA (10 μg/ml), MDP (10 μg/ml), or heat-killed bacteria (multiplicity of infection (MOI) = 100) for 24 h. Culture supernatants were collected, passed through 0.22-μm pore size filters, and then stored at −80°C until the cytokine assay.

Isolation of colonic lamina propria Mϕ (CLPMϕ) and splenic Mϕ

Lamina propria mononuclear cells were isolated using a modified protocol as previously described (25). Briefly, mice were sacrificed, and colonic tissues were removed. Isolated colons were washed with HBSS, dissected into small pieces, and incubated in HBSS containing 2.5% FBS and 1 mM DTT (Sigma-Aldrich) to remove any mucus. Then, the pieces were incubated in HBSS containing 1 mM EDTA (Sigma-Aldrich) twice for 20 min each at 37°C, washed three times with HBSS, and incubated in HBSS containing 1 mM collagenase type IV (Sigma-Aldrich) for 2 h at 37°C. Digested tissues were filtered and washed twice with HBSS. Isolated cells were resuspended in 40% Percoll (Pharmacia Biotech), layered onto 75% Percoll, and centrifuged at 2000 rpm for 20 min. Cells were recovered from the interphase and washed with PBS. CLPMϕ and splenic Mϕ were purified by positive selection from lamina propria mononuclear cells or unfractionated splenocytes using MACS CD11b microbeads (Miltenyi Biotec) as previously described (24, 26).

Activation of Mϕ by whole bacteria Ags

BM-derived Mϕ, and isolated CLPMϕ and splenic Mϕ were plated on 96-well tissue culture plates (1×10^5 cells/well) in RPMI 1640 medium supplemented with 10% FBS and antibiotics, and stimulated by heat-killed bacterial Ags (MOI = 100) for 24 h at 37°C. Culture supernatants were collected, passed through a 0.22-μm pore size filter, and stored at −80°C until the cytokine assay.

Cytokine assay

A mouse inflammatory cytometric beads array (CBA) kit (BD Pharmingen) was used for cytokine measurements, according to the manufacturer's instructions. Samples were analyzed using a FACSCalibur (BD Pharmingen).

Quantitative RT-PCR

After 8 h of stimulation by bacterial Ags, total RNA was isolated from Mϕ using an RNeasy Mini kit (Qiagen). In some experiments, RNA was isolated from colonic tissues and spleen. cDNA was synthesized with OmniScript reverse transcriptase (Qiagen). For quantitative RT-PCR, TaqMan Universal PCR Master Mix and TaqMan Gene Expression Assays for murine IL-12p35, IL-12p40, IL-23p19, M-CSF, GM-CSF, and β-actin (Applied Biosystems) were used. PCR amplifications were conducted in a thermocycler DNA Engine (OPTICON2; MJ Research). Cycling conditions for PCR amplification were 50°C for 2 min and 95°C for 10 min, followed by 40 cycles of 95°C for 15 s and 60°C for 1 min.

Statistical analysis

Statistical significance of differences between two groups was tested using a Student's *t* test. For comparison of more than two groups, ANOVA was used. If the ANOVA was significant, Dunnett's multiple comparison test or Scheffe's test were used as a post hoc test.

Results

GM-Mϕ and M-Mϕ derived from BM $CD11b^+$ cells from IL-$10^{-/-}$ mice do not differ significantly from those derived from WT mice in morphology and cell surface Ag expressions

When BM-derived $CD11b^+$ cells from WT mice were cultured in M-CSF or GM-CSF for 7 days, they showed morphological

changes characteristic of Mϕ such as increases in size and adherence, and were stained with nonspecific esterase (data not shown). As shown in Fig. 1*A*, GM-CSF and M-CSF induced differentiation of BM CD11b$^+$ cells into two distinct subsets of adherent Mϕ, which corresponded to human GM-Mϕ and M-Mϕ (27). GM-Mϕ derived from BM CD11b$^+$ cells had a rounded morphology and possessed dendrites, similar to DCs. In contrast, M-Mϕ derived from BM CD11b$^+$ cells had an elongated spindle-like morphology. FACS analysis revealed that GM-Mϕ expressed higher levels of MHC class II molecules and costimulatory molecules CD80 compared with M-Mϕ (Fig. 1*B* and Table I). Expression of Gr-1 was also different between them; i.e., GM-Mϕ but not M-Mϕ expressed Gr-1 (Fig. 1*B* and Table I). However, CD11c, a DC marker, was not expressed on both Mϕ (data not shown).

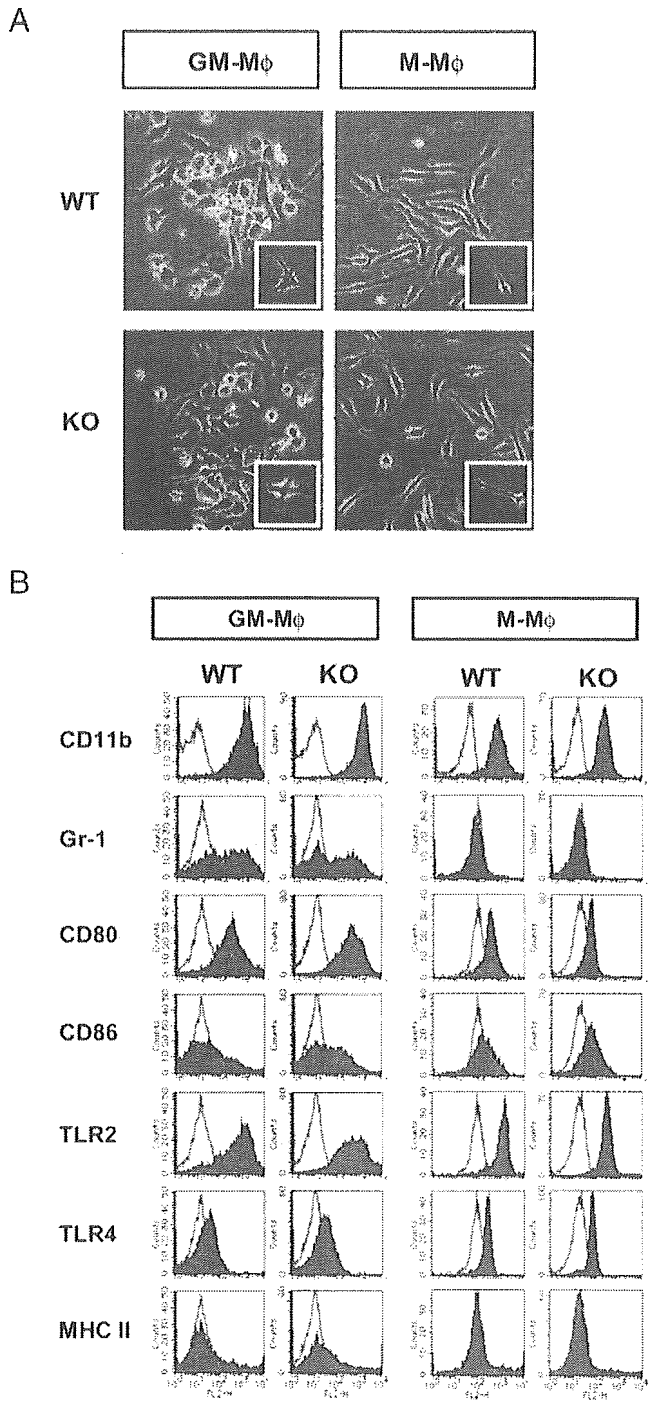

FIGURE 1. In vitro differentiated Mϕ from WT and IL-10$^{-/-}$ mice do not differ in morphology and surface marker expressions. *A*, BM CD11b$^+$ cells from WT and IL-10$^{-/-}$ mice were polarized into Mϕ with GM-CSF or M-CSF for 7 days. *B*, Polarized Mϕ from WT and IL-10$^{-/-}$ mice (KO) were stained with the indicated mAbs and analyzed by flow cytometry. Profiles of specific Ab staining (shaded histograms) and staining with isotype controls (open histograms) are shown. Data shown are representative of five independent experiments.

Next, we compared the two Mϕ subsets derived from IL-10$^{-/-}$ BM CD11b$^+$ cells with those from WT BM CD11b$^+$ cells. As shown in Fig. 1*A*, both GM-Mϕ and M-Mϕ from IL-10$^{-/-}$ BM CD11b$^+$ cells showed normal morphological characteristics. Flow cytometric analysis further revealed that these Mϕ subsets from IL-10$^{-/-}$ mice did not differ from those in WT mice in their cell surface Ag expressions (Fig. 1*B* and Table I). These results suggest that GM-Mϕ and M-Mϕ from IL-10$^{-/-}$ mice are similar to those in WT mice, at least in terms of morphology and cell surface Ag expression.

BM-derived M-Mϕ from WT mice show an anti-inflammatory phenotype in response to PAMPs and whole bacterial Ags

To determine the immunological responses of GM-Mϕ and M-Mϕ from WT mice to PAMPs stimulation, Mϕ were stimulated with various kinds of PAMPs for 24 h, and production levels of IL-12p70 and IL-10 in culture supernatant were measured. As shown in Fig. 2*A*, none of the stimuli tested induced IL-12p70 production from both Mϕ in WT mice. In contrast, the TLR4 ligand LPS, TLR2 ligands PGN and Pam_3CSK_4, and TLR9 ligand *E. coli* ssDNA induced IL-10 production by these Mϕ, although the amounts produced were higher in M-Mϕ compared with GM-Mϕ. The NOD2 ligand MDP did not induce either IL-12p70 or IL-10 in either subset from WT mice.

Next, we examined the effects of whole bacterial Ags on these Mϕ. In contrast to stimulation with PAMPs, stimulation of GM-Mϕ with heat-killed *E. coli* and *E. faecalis* induced IL-12p70 production (Fig. 2*B*). However, M-Mϕ from WT mice did not produce IL-12p70, but did produce large amounts of IL-10 in response to the whole bacterial Ags (Fig. 2*B*). These results suggested that M-Mϕ, but not GM-Mϕ, in WT mice act as anti-inflammatory Mϕ in the recognition of bacteria.

BM-derived M-Mϕ but not GM-Mϕ from IL-10$^{-/-}$ mice reveal abnormal hyperproduction of IL-12 and IL-23 in response to whole bacterial Ags

We next examined the effects of PAMPs and whole bacteria Ags on GM-Mϕ and M-Mϕ from IL-10$^{-/-}$ mice. In contrast to the results obtained from Mϕ in WT mice, IL-10$^{-/-}$ Mϕ produced IL-12p70 by stimulation with LPS or Pam_3CSK4, although the amounts were very low, and no significant differences were observed between GM-Mϕ and M-Mϕ (Fig. 3*A*). The use of 10-fold higher concentrations of these PAMPs did not induce higher levels of IL-12p70 either (data not shown).

Upon whole bacteria stimulation, such as with heat-killed *E. coli* and *E. faecalis*, GM-Mϕ from IL-10$^{-/-}$ mice produced similar levels of IL-12p70 to WT GM-Mϕ, although they lacked IL-10 production ability (Fig. 3*B*). Surprisingly, in contrast to WT M-Mϕ, M-Mϕ from IL-10$^{-/-}$ mice produced significantly large amounts of IL-12p70 upon stimulation with whole bacterial Ags (Fig. 3*B*). In addition, a lower dose of the whole bacteria Ag (MOI = 10) also induced abnormally large IL-12p70 production (data not shown).

To further confirm this abnormal IL-12p70 hyperproduction by IL-10$^{-/-}$ M-Mϕ, gene transcriptions of IL-12p35, p40, and IL-23p19 were analyzed using real-time quantitative PCR. Results revealed that basal expressions of these genes before stimulation